Universidade do Algarve

Departamento de Ciências Biomédicas e Medicina

Phenotypic Study of Mutant Embryos for the Gene ADTK1 in Mice

Nídia Sofia Maltez Cunha

Tese Orientada por Professor Doutor José António Belo

Mestrado em Ciências Biomédicas

Biologia do Desenvolvimento Embrionário

Setembro de 2011

Dissertação de Candidatura ao Grau de Mestre em Ciências Biomédicas, Área de Biologia do Desenvolvimento pela Universidade do Algarve

Master Thesis proposal in Biomedical Science, Developmental Biology by the University of Algarve

As opiniões expressas nesta publicação são da exclusiva responsabilidade do seu Autor.

The contents of this dissertation are of the exclusive responsibility of this Author.

(Nídia Sofia Maltez Cunha)

Podemos nunca

vir a saber que resultados

produz a nossa acção.

Mas, se nada fizermos,

não haverá resultados.

Mahatma Gandhi (1869-1948)

DEDICATION

To my mother and father, and my brother.

Thank you for your patience, love and support!

Acknowledgments/Agradecimentos

Para começar, gostaria de agradecer em primeiro lugar ao meu orientador, Professor Doutor José António Belo, por me ter dado a oportunidade de realizar este trabalho, no seu laboratório, com a sua equipa fantástica e com o seu apoio. Por todos os esclarecimentos, conselhos, compreensão nos momentos de decisões difíceis e apoio prestado ao longo destes anos.

Queria também agradecer ao Centro de Biomedicina Molecular e Estrutural (CBME) pelo acolhimento e pelas óptimas condições de trabalho que nos oferece, por todo o apoio que me foi prestado e que possibilitou a elaboração deste trabalho.

Gostaria muito de agradecer a todos os meus colegas de laboratório, são uma equipa fantástica que muito me ajudou na realização de algumas experiências efectuadas para esta tese, com um bom espírito de equipa e trabalho e interajuda ainda me forneceram um ambiente muito agradável.

Um forte agradecimento à Marta por todo o ensino, ajuda e compreensão. Foi ela que me amparou nas situações mais difíceis de ultrapassar. Sem a sua ajuda não conseguiria escrever esta tese. À Carolina, "piriga" terrível, por toda a ajuda e ensinamentos, por todas as caminhadas ao biotério e pelas famosas limpezas de gaiolas. Ao Zé, ou melhor, ao "Tio Zé" pelas críticas construtivas constantes e pela leitura desta tese. Ao segundo tio, João Facucho por todas as ideias partilhadas pela manhã. À Marisa por todo o seu "tchanam", é sem dúvida uma pessoa única. À Margaret por todos os conselhos e por ser muito querida comigo. À Rubi e ao João Furtado por toda a sua amizade e carrinho. A Sara e à Betty que sempre que as solicitei me ajudaram muito. As vizinhas do laboratório da frente, à Mónica e à Marinella por toda a amizade. À Lisa pelo trabalho que teve na construção genética do ratinho que foi o meu objecto de estudo. E por último aos meus "companheiros de guerra", ao Fernando Cristo e ao João Baptista por todos os bons momentos que ultrapassamos juntos na UAlg onde nos conhecemos. Obrigado por todo o apoio, por todas as festas e todos os sorrisos ao longo destes anos. A todos desejo-lhe as maiores felicidades.

E por último agradeço às pessoas mais importantes, à minha família. Em primeiro lugar aos meus pais, os meus pilares de apoio. Sem vocês nunca teria chegado onde estou hoje, pois não sei se teria coragem de seguir em frente. À minha mãe por sempre ter acreditado, valorizado e apostado na sua filhota. Por todo o amor, carrinho e tempo que dedicou na minha formação. Ao meu pai por sempre ter vivido em prol da família que tanto ama. Por todo o apoio, compreensão, dedicação e sacrifícios. Ao maninho que tanto amo, por sempre me ter dado força. Com a sua presença torno-me mais forte e madura. Por todas as horas perdidas serem recompensadas com o seu crescimento. As minhas madrinhas, Leonor e Bia. À Leonor por toda a ajuda, conselhos e apoio nos momentos difíceis e de indecisões, apesar da distância está sempre presente. À Bia por ter estado constantemente envolvida no meu crescimento, sempre pronta a fazer as minhas vontadinhas desde pequena como que a avó que já não tenho. À restante família, pois a minha família é base de tudo o que sou e de todo o que consegui até hoje.

Ao Carlos por todo o seu amor, carrinho, compreensão e ajuda nos "painéis fotográficos". Por todas as noites que me acompanhaste ao laboratório para eu não estar lá sozinha.

A todos os meus verdadeiros amigos, obrigado por todo o apoio em tudo o que preciso.

À Sofia por toda a compreensão, ajuda e "traduções". Sem a tua paciência não conseguiria escrever esta tese.

Agradeço ainda a todas as restantes pessoas que não mencionei e que contribuíram para a conclusão desta tese de mestrado.

Abstract

A differential screening conducted to identify novel genes expressed in the anterior visceral endoderm (AVE) led to the isolation/identification of *Adtk1,* a gene coding for a protein with tyrosine and serine/threonine kinase domains. The analysis at birth of generated *Adtk1* mouse mutants has been reported by our and other laboratories. Several defects were identified, namely the mutants were slightly smaller and had limbs with shortened long bones than wild-type littermates.

In the course of this thesis it was observed that inbreeding *Adtk1* mutation into the C57Bl6 background resulted in embryonic death identified by genotyped *conceptus,* suggesting the importance of this gene along the embryonic development.

A more in-depth analysis of this mutation in mixed background (C57Bl6/DBA) revealed that *Adtk1*$^{-/-}$ animals also presented kidney defects. Furthermore, preliminary analysis of E9.5 *Adtk1* KO embryos in a pure inbred background (C57Bl6) revealed that they display severe defects associated with neural tube closure.

Keywords: *Adtk1*, Bone Formation, Embryonic Development, Kidney, Mouse, Neural Tube, PCP.

Resumo

Com o objectivo de caracterizar e melhor compreender o papel da endoderme visceral anterior ao longo do desenvolvimento embrionário de ratinho, tendo em conta os genes que nela são expressos, no nosso laboratório foi realizado um *screening* diferencial. No decorrer desse *screening* foram seleccionados genes que se encontram sobre expressos na região da endoderme visceral anterior. Vários novos genes foram identificados e entre estes encontrava-se o *Adtk1* (Anterior Distal Tyrosine Kinase 1). O gene *Adtk1* foi então isolado e caracterizado.

No nosso laboratório demonstrou-se que o gene *Adtk1* está expresso desde muito cedo no desenvolvimento embrionário e permanece expresso durante toda a fase embrionária. Desde o início, a análise padrão de expressão sugeriu um papel importante para *Adtk1* durante o desenvolvimento embrionário. Devido a esse facto foi feita uma inactivação deste gene em ratinho através de recombinação homóloga. Após a obtenção dos primeiros animais heterozigóticos para o gene Adtk1 realizaram-se os primeiros estudos preliminares, publicados em Gonçalves, et al (2011). Além do nosso laboratório também outros dois grupos de investigação realizaram o estudo do gene *Adtk1*, Imuta, et al (2009) e Kinoshita, et al (2009). Após a análise preliminar e as publicações o nosso laboratório continuou então o estudo do gene *Adtk1*.

O trabalho apresentado nesta tese concentrou-se na continuação do estudo do gene *Adtk1*. A fim de entender melhor o fenótipo obtido na ausência do gene *Adtk1* durante o desenvolvimento de ratinho, vários tipos de experiencias foram realizadas e relatadas neste manuscrito.

O gene *Adtk1* codifica uma proteína com domínio catalítico tirosina/serina/treonina cinase. Uma vez que este gene é sobre expresso na região da endoderme visceral anterior, região que contém tantos genes de particular interesse para os vários processos essenciais à embriogénese, seria de todo o interesse realizar-se uma análise do fenótipo de ratinhos com o gene *Adtk1* inactivado (KO), durante as várias fases do desenvolvimento embrionário.

Para a análise do fenótipo de ratinhos *Adtk1*$^{-/-}$ cruzaram-se animais heterozigóticos, *Adtk1*$^{+/-}$C57BL6. Contudo, não obtivemos qualquer ratinho KO na fase de recém-nascido. Tal facto levou-nos a suspeitar que uma morte intra-uterina poderia estar a ocorrer. Para testar esta hipótese começou-se a dissecar fêmeas durante o desenvolvimento embrionário, mas a suspeita da existência de morte intra-uterina começou a ser confirmada, através da presença de decíduas vazias (placenta, onde o embrião morto é reabsorvido pela mãe) em todas as ninhadas dissecadas. Devido a essa suspeita começamos a dissecar fêmeas ao longo de vários estádios do desenvolvimento embrionário. Começamos pelo E13.5, E12.5 e E10.5 na esperança de encontrar embriões *Adtk1*$^{-/-}$,todavia a ausência destes embriões manteve-se. Assim sendo, continuámos a dissecar embriões a estádios menos desenvolvidos e observamos mais uma vez a existência de decíduas vazias em quase todas as fêmeas dissecadas. Isso indicava que o mais provável era os embriões estarem a morrer mais cedo do que o estádios analisados até ao momento. Fomos dissecando cada vez mais cedo e a E9.5 encontramos o primeiro embrião *Adtk1*$^{-/-}$. Este embrião demonstrava más formações ao nível do fecho do tubo neural.

Análise preliminar de embriões E9.5 *Adtk1*$^{-/-}$ na estripe C57BL6 pura revelou defeitos graves associadas ao fecho do tubo neural. Estes resultados são ainda apoiados por experiencias realizadas utilizando *Xenopus leavis* onde a ausência dos genes ortólogos de *Adtk1* durante o desenvolvimento induz defeitos na migração celular durante o fecho do tubo neural e gastrulação (M. Vitorino, não publicado). Assim sendo, é possível que o *Adtk1* também esteja envolvido no fecho do tubo neural durante o desenvolvimento dos vertebrados.

Durante as dissecções a menores estádios de desenvolvimento foi encontrado um embrião *Adtk1*$^{-/-}$ a E8.5, em poucos embriões dissecados nesta fase. O único embrião *Adtk1*$^{-/-}$ encontrado não se revelou ser esclarecedor, uma vez que estava muito deformado, não nos permitiu identificar as diferentes estruturas que constituem

o embrião. No entanto, este é um resultado preliminar que precisa ser analisado através da dissecação de mais embriões nesta fase.

Posteriormente, procedeu-se a mais dissecações em estádios mais iniciais e até à data apenas dois embriões *Adtk1*$^{-/-}$ foram encontrados em E6.5. Tais embriões não parecem revelar uma grande diferença em comparação com os embriões do tipo selvagem no mesmo estádio. Assim, seria muito importante analisar as migrações ocorridas nestas etapas. Em *Xenopus leavis*, observamos que na ausência dos ortólogos de *Adtk1*, o fecho do blastóporo estava atrasado (Marta Vitorino, não publicado). Por isso, deve ser estudado se o mesmo tipo de problemas na migração de células está a ocorrer em embriões *Adtk1*$^{-/-}$ de ratinho durante o desenvolvimento inicial, E5.5-E6.5, e avaliar se a adequada migração celular da endoderme visceral distal para originar a endoderme visceral anterior está a ocorrer em mutantes *Adtk1*.

Os estudos efectuados numa estirpe híbrida (C57BL6) indicaram-nos uma muito baixa percentagem de embriões *Adtk1*$^{-/-}$. Como os recém-nascidos analisados por outro grupo de investigação tinham um fundo híbrido (estirpes CBA e C57BL6, nós na tentativa de obter recém-nascidos *Adtk1*$^{-/-}$ decidimos gerar um fundo híbrido. Para esse efeito, cruzamos ratinhos *Adtk1*$^{+/-}$ C57BL6 com ratinhos DBA do tipo selvagem. A partir deste cruzamento obtivemos a geração F1, *Adtk1*$^{+/-}$C57BL6;DBA. Na idade adulta, os ratinhos heterozigoticos foram cruzados entre si resultando assim a geração F2. Esta geração foi recolhida logo após o nascimento e analisada em busca de ratinhos *Adtk1*$^{-/-}$ através de genotipagem.

Com um background misto obtivemos 2 recém-nascidos *Adtk1*$^{-/-}$. Estudos preliminares utilizando estes ratinhos (C57Bl6/DBA), demonstraram que os rins de ratinhos *Adtk1*$^{-/-}$ apresentavam um córtex e uma zona glomérular com alterações estruturais e morfológicas em análise histológica. Como anteriormente já tínhamos determinado que *Adtk1* é expresso nos rins do ratinho durante o desenvolvimento embrionário (de E12.5 até ao nascimento), os resultados obtidos no fundo misto, numa análise preliminar, sugerem que a expressão do gene *Adtk1* poderá ser muito

importante para o desenvolvimento apropriado do rim. Todavia, o desenvolvimento do rim é um processo ainda não totalmente compreendido. Sabe-se que as moléculas de várias vias de sinalização estão envolvidas na formação do rim, no entanto, as suas posições relativas nas vias permanecem pouco conhecidas e alguns dos seus intermediários permanecem ainda por desvendar. Contudo, para melhor compreender a expressão do gene *Adtk1* no decorrer do desenvolvimento embrionário renal, hibridações *in situ* para este gene e marcadores renais conhecidos foram feitas.

Dados apresentados por Imuta, et. al. (2009), mostraram que ratinhos *Adtk1*$^{-/-}$ (*Pkdcc*) recém-nascidos apresentavam membros mais curtos do que os recém-nascidos do tipo selvagem. O esqueleto dos mutantes *Adtk1* recolhidos após o nascimento foi analisado e também apresentava diferenças no comprimento do osso, embora mais ténues em comparação com as diferenças encontrada por Imuta et al (2009).

Podemos também afirmar que há vantagens e desvantagens em realizar a primeira análise de um ratinho KO sobre um fundo genético misto. No entanto, recentemente no nosso laboratório após esta mutação estar num fundo puro C57BL6, fomos capazes de demonstrar a importância deste gene ao longo do desenvolvimento embrionário, o que foi evidenciado pela morte embrionária nas dissecções genotipadas. Também mostramos os possíveis defeitos que ocorrem em estádios iniciais de desenvolvimento embrionário em estirpe pura.

No final desta tese de mestrado, algumas de nossas questões iniciais foram respondidas, enquanto outras permaneceram sem resposta. Neste momento, pensamos que ainda há muito trabalho a ser feito a partir destes dados preliminares.

Palavras-chave: *Adtk1*, Desenvolvimento Embrionário, Formação Óssea, PCP, Ratinho, Rins, Tubo Neural.

Abbreviations

3'	**3 prime**
5'	5 prime
µL	Microliter
µm	Micrometer
aa	Amino acid
Ab	Antibody
ADE	Anterior Definitive Endoderm
Adtk1	Antero Distal Tyrosine Kinase 1
AER	Anterior Ectodermal Ridge
AP	Anterior-Posterior
ASE	Asymmetric Intronic Enhancer
AVE	Anterior Visceral Endoderm
BMP	Bone Morphogenetic Protein
bp	Base pair
cDNA	Coding Deoxyribonucleic Acid
CDS	Coding Sequence
Cerl	Cerberus-like
Chd	Chordin
CNS	Central Nervous System
DEPC	Diethyl pyrocarbonate
Dhh	Desert hedgehog
DIG	Digoxigenin
Dkk	Dickkopf
DLHP	Dorsolateral hinge point
DMEM	Dulbecco's Modified Eagle Medium
DNA	Deoxyribonucleic acid
Dpc	Days post coitum
DV	Dorso-Ventral
DVE	Distal Visceral Endoderm
E	Embryonic day
EGO	Early Gastrula Organizer
EPI	Epiblast
ER	Endoplasmatic Reticulum
ES	Embryonic stem
EtBr	Ethidium bromide
FBS	Fetal Bovine Serum
FD	Faraday
FGF	Fibroblast growth factor
Fw	Forward
Fz	Frizzled
h	Hour
ICM	Inner Cell Mass
Kb	Kilo base
Ko	Knock-out

JNK	Jun-N terminal Kinase
LPM	Lateral Plate Mesoderm
L-R	Left-Right
LRP	Low-density-lipoprotein Receptor-related Protein
M	Molar
MAP	Mitogen-Activated Protein
MEF	Mouse Embryonic Fibroblast
Mg	Milligram
MGO	Mid Gastrula Organizer
MHP	Medium hinge point
min	Minute
mL	Milliliter
mRNA	Messenger Ribonucleic Acid
NTD	Neural tube defect
Oep	One eye pinhead
ON	Overnight
Otx2	Orthodenticle-related homeobox
PBS	Phosphate-buffered saline
PCP	Planar Cell Polarity
PCR	Polymerase Chain Reaction
P-D	Proximal-Distal
PE	Primitive Endoderm
PFA	Paraformaldehyde
PKC	Protein Kinase C
p.m.	
PSM	Presomitic Mesoderm
Ptc	Patched
RA	Retinoic acid
Rev	Reverse
RNA	Ribonucleic acid
RT	Reverse Transcription
RT	Room Temperature
RTK	Receptor tyrosine kinases
SDS	Sodium dodecyl sulfate
SFRP	Secreted Frizzled Related Protein
Shh	Sonic hedgehog
SMART	Simple Modular Architecture Research Tool
Smo	Smoothed
TE	Trophoectoderm
TGF-β	Transforming Growth Factor-Beta
UTR	Untranslated Region
UV	Ultraviolet
V	Volt

VE	Visceral Endoderm
WISH	Whole mount in situ hybridization
Wt	Wild-type
ZPA	Zone of Polarizing Activity

Índice

List of Figures

Introduction

1.1 Research in Developmental Biology

Developmental biology is the discipline that studies the process that occurs from having a single cell (the fertilized *ovum*) to complex cellular networks that give rise to the highest levels of complexity of the organism. It involves using complex tools such as gene induction and repression, tissue specialization, gene allocation and gene interactions.

Understanding the pathways on how this fundamental problem is solved is a topic of many projects in developmental biology. They include early pattern formation, the development of cell types and organ systems including the nervous system and the evolution of developmental mechanism, aging and senescence, and stem cells in developmental biology and medicine.

Many research groups are focused on the field of pattern formation, namely in the communication between cells and within cells. This is a central role in developmental biology research with major relations to quantitative and modeling approaches. The communication between cells is required and the respective (despite the fact that the form of an organism is already preprogrammed in its DNA) pathways are mediated by signaling molecules, which are released by signaling centers that organize other cells within a tissue or an organism. These signaling centers play a major role in embryogenesis and regeneration.

The origin of an individual organ during the development, organogenesis, also involves general rules that can be genetically dissected in various model systems It is a challenge to model these rules on a theoretical level and to understand on the molecular level how they contribute to form the many cell types that make up a complex organism.

Developmental Biology is not only the Science that understands embryology and cell differentiation, it is also the basic science that understands human cancer, aging and the prerequisites for regenerative medicine.

1.2 - Animal Models

The major aim in genetic research is to understand the biological mechanisms of human development and disease. In many cases, however, there are both logistical and ethical issues involving studies in a human system. To overcome that barrier, a variety of animal models for genetic and functional studies relevant to human biology have been commonly used in the past years. Actually, technical developments that allow the manipulation of gene expression, coupled with the ongoing acquisition of genomic sequences, have enhanced the usefulness of animal models and assured their importance for the functional characterization of the human genome.[2]

1.2.1 – Mouse (*Mus musculus*) as Animal Model

The importance of mouse, *Mus musculus*, for the research in biomedical science is crucial because it is an excellent model organism for the study of genetics and development in vertebrates and it has a pivotal role in the study of mammalian development, physiology and biochemistry. At the turn of the twentieth century, genetic investigations of mouse mutations were initiated, shortly after the discovery of Mendel's laws.[3] Its small size, modest cost, readily adaptation to laboratory conditions combined with a relatively short breeding cycle (approximately 8 weeks with a gestation time of 21 days and 4–6 weeks to maturity) make it an attractive model for both development and physiological studies, and very important for genetic analysis[1].

Probably the most important factor contributing to the use of mouse as a genetic model was the development of several, fully inbred, genetically homogenous mouse strains, such as the C57BL/6, DBA/2 and BALB/C lines (Figure 1).[4] The

development of technologies to manipulate the mouse germ line by transgenesis or homologous recombination has made mouse once again the definitive system for studying mammalian gene function.[5] These genes alter the phenotypic consequences of mutations of other genes. Their importance has become obvious as investigators have learned that the phenotype of many engineered or spontaneous mutations can be influenced by genetic background.[6] This is of particular importance for mutations that are models of human diseases and the identification of modifiers that influence the severity or progression of a disease has potential as a target for therapeutic intervention. More than 700 mutant strains are also available for study and these strains involve almost every aspect of development and metabolism, such as coat colour, skeletal structure, hematology, endocrine and immune systems, neurological and behavioral characteristics, and viral, disease and tumor susceptibility or resistance. This gathering of developmental, physiological and genetic studies has turned it into the leading organism for the study of human disease, and in particular disease with an underlying genetic basis.

Figure 1: Different strains of Mus musculus. (Adapted from the journal Genome Research August 2004 Volume 14 Number 8)

1.3 - Mouse Embryogenesis

1.3.1 - Early Mouse Development

In mammals, development begins with a sequence of mitosis followed by the separation of cells originating the embryo from cells providing support to the embryo itself during pregnancy.[7] Proliferation, differentiation, migration and apoptosis are the cellular processes underlying development.[7] These events occur according to a specific temporal and spatial program, driven by the architectural plan for each body structure.[8]

Embryonic development in the mouse begins at fertilization. Mouse mating usually takes place at night. When the plug is found the next morning, it is recorded as 0.5 d.p.c (0.5 days post-coitum, or E0.5, embryonic day 0.5) meaning that fertilization is occurred half a day previously. A litter of pups is born in the morning of 18-19.5 d.p.c. and traditionally, the gestation period in mice is considered to be 19.5 days (Figure 2).

Embryogenesis and fetal growth from fertilization to birth can be divided into six stages, each one featuring one or more special events (Figure 2). The seven stages

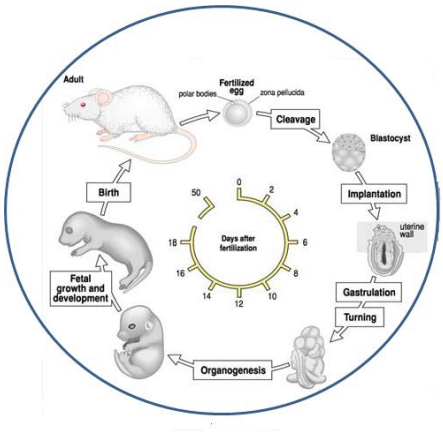

Figure 2: Mice life cycle. Embryogenesis and fetal growth from fertilization to birth can be divided in six stages: cleavage, implantation, gastrulation, turning, organogenesis and fetal growth and development. (Adapted from Principles of Development, Wolpert et al, 1998)

include cleavage, implantation, gastrulation, turning, organogenesis, and fetal growth and development.[7]

1.3.1.1 Fertilization, Pre-implantation and Implantation

Fertilization is a multistep process. In mouse, male and female pronuclei, containing the haploid chromosomes of the sperm and egg, respectively, form during the one-cell zygote stage and migrate towards each other undergoing DNA replication at the same time. [7]First, sperm must bind to the egg protective membrane, the *zona pellucida*, which is a thick solid shell, made of glycoproteins.[7] In the process of binding to the egg membrane, the sperm releases special proteases that provide it with the ability to penetrate its way through the *zona pellucida* into the space that surrounds the egg membrane.[8] Although multiple sperm can make it into this space, only one can fuse with the egg.[8] Egg and sperm fusion causes fast electrochemical changes in the egg membrane that prevent the entry of additional sperm.[9] The fusion event also makes the newly fertilized egg to move down the pathway of animal development.[9]

The fertilized mouse egg is a small (approximately 80 µm in diameter) cell. It has polarity, because the polar bodies generated by the first and second meiotic divisions are sequentially extruded at the same site, where they remain tethered during ensuing cleavage (Figure 3). [10]

Fertilization of the egg inside the ampulla of the oviduct will activate to initiate pre-implantation development.[11] The control lineage segregation in the fertilized egg is essential to understand normal mammalian development.[12] Even though cleavage stages are prolonged, taking approximately 3 days for the egg to produce 16 cells, the zygotic genome is activated and maternal mRNA degraded at the two cell stage, within 24 hr of fertilization.[11]

1.3.1.2 Pre-implantation

The initial pre-implantation events are controlled by maternal molecules. [13] Throughout the cleavage stage, all of the cells in the developing embryo are equivalent and totipotent, since they have not yet undergone differentiation and still retain the ability to produce every cell type present in the developing embryo and adult animal [1]. As a consequence of totipotency, cleavage stage embryos can be reduced to smaller groups of cells that each have the potential to develop into individual animals[1].

Figure 3: First cleavages and pre-implantation in mouse embryo. Left to right: 2-cell, 8-cell, early blastocyst, and late blastocyst. In the late blastocyst, cells have committed to the trophectoderm (future placenta) and inner cell mass (future body) lineages. (Adapted from Vernadeth B. Alarcon http://www3.jabsom.hawaii.edu/Grad_DRB/faculty/alarcon.html (consulted in 4 of September of 2011))

From third to eighth cell, cycles of pre-implantation development are shorter and take place as the embryo moves down the coiled oviduct to enter the uterine lumen, finally to hatch from the *zona pellucida* by enzymic activity and to adhere to the uterine endometrium and implant.[1]

These cleavages take around five days from fertilization and then the formation of the late blastocyst occurs, during which the fertilized egg undergoes 5 cleavages to reach a solid ball of 32 cells called the morula.[14] The morula cells make a two-lineage commitment to form the early blastocyst, which continues development to the late blastocyst stage prior to implantation.[14] At this stage the cells undergo a dramatic change in their behavior, through a mechanism called compaction, which consist on the increasing of contacts of the outer cells of the morula with one another by tight junctions and closing the inside of the sphere.[7] This phenomenon creates conditions

to separate the trophoblast or trophoectoderm (the external cells of the morula) from the internal cells, the inner cell mass (ICM).[14]

The cells of the trophoblast secrete fluid into the morula and create a blastocoel and the ICM. This structure, ICM, becomes localized in one side of the ring of trophoblast cells, generating the structures named blastocyst.[15] The blastocyst is a spherical cyst, formed from the 32-cell stage (E3.5) and composed of an outer polarized epithelial monolayer, the trophectoderm, an inner cluster of nonpolarized cells, the ICM, and the blastocoel cavity, adjacent to the ICM (Figure 4).[15] The primitive endoderm will contribute to parietal and visceral endoderm. It differentiates on the surface of the ICM and includes one cell layer which is in contact with the blastocoel cavity.[8]

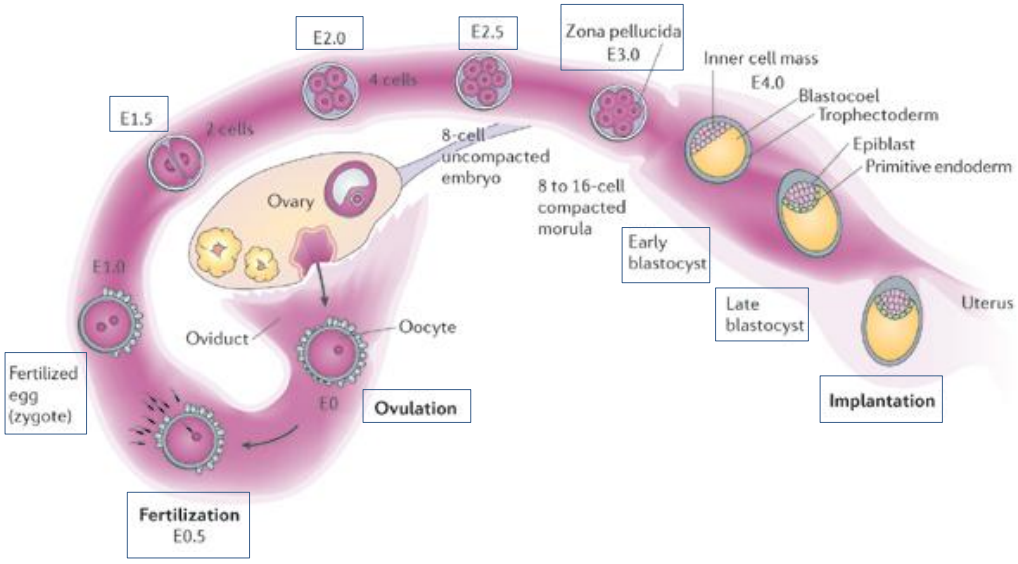

Figure 4: Pre-implantation and implantation in mice embryo development. After fertilization in the oviduct, the embryo experiences numerous sequences of mitotic cell division, finally forming a ball of cells named morula. The embryo enters the uterine lumen at the late morula stage, and transforms into a blastocyst that holds a cavity (named blastocoel) with two different cell populations, the inner cell mass (ICM) and the trophectoderm (the progenitor of trophoblast cells). Previously to implantation, the blastocyst goes from its outer shell (the zona pellucida) and differentiates to generate additional cell types — the epiblast and the primitive endoderm. At this stage, the trophectoderm connects to the uterine lining to beggin the process of implantation. E stands for embryonic day (Adapted from Wang and Dey 2006 [1])

The trophoblast cells produce no embryonic structures, instead they form the chorion and the embryonic portion of the placenta. The ICM will give rise to the embryo and its associated yolk sac, allantois and amnion.[8] At the 64-cell stage, the ICM and the trophoblast cells have become separated cell layers.[9] The ICM actively supports the trophoblast, secreting proteins such as Fgf4 that make the trophoblast cells divide. [8]

The hypoblast (primitive endoderm) is an epithelial layer comprising about 20 cells that commences differentiation just prior to blastocyst implantation at 4–4.5 days post-fertilization from ICM cells adjacent to the blastocoelic cavity (Figure 4).[14] The remaining ICM cells at this time are known as the epiblast (primitive ectoderm).[16] The core of the ICM will develop into the epiblast, the progenitor tissue for the whole animal (Figure 5)[9].

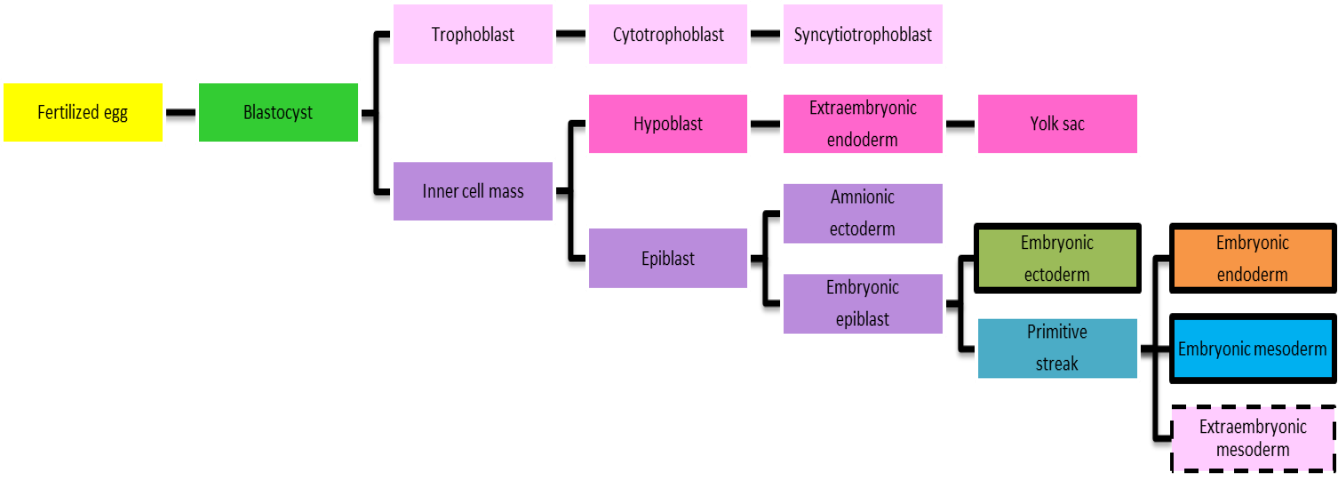

Figure 5: Schematic diagram demonstrating the tissue derivation in mouse. The future extraembryonic tissues are represented in pink. The embryonic tissues are represented by the boxes limited in black. The extraembryonic mesoderm, represented by the box limited in black strips, may have two possible origins, the primitive streak or the yolk sac. Adapted from [1]

1.3.1.3 Uterine Implantation

In order to proceed with development, the blastocyst must implant in the uterine wall. The mouse embryo implants, at stage 4.5, and during the immediate post-implantation (E5.0-E6.0) the embryonic tissue volume increases around 40 fold.[16]

Interactions between the late blastocyst and the uterine wall trigger the mural trophectoderm to differentiate into trophoblast giant cells and the polar trophectoderm to form the ectoplacental cone (Figure 4).[15]

The first 4.5 days of mouse development result in the formation of three mutually exclusive tissue lineages: the trophectoderm, the primitive endoderm and the epiblast (Figure 4).[15]

Implantation is completed by E5.5 and the embryo joins the mother in the uterine wall like a bean bud spouting in the soil. The epiblast elongates and an internal cavity is developed giving it a cup-shaped form (Figures 3, 4).[15] The development of the embryo progresses to the egg cylinder.[17];[7] The cavity formation is possibly the first apoptotic event in mouse development.[15]

Originally, the epiblast is a solid structure of cells. During early embryogenesis, signals trigger the cells in the center to die creating a hollow structure (Figure 4).[7]

1.3.2 Gastrulation: Post-Implantion

In the early post-implantation of mouse embryo there is a gastrulation stage, which involves changes in cell mobility, cell shape and cell adhesion.[1] This stage is a morphogenetic process that converts the epiblast into the three primary germ layers: endoderm, mesoderm and ectoderm, from which all the fetal tissues will develop. Together these layers form the basic body plan of the fetus, evident by about E8.5.[7] The ectoderm will generate skin and the nervous system, the mesoderm will give rise to the blood, bone and muscle and the endoderm will originate the respiratory and digestive tracts (figure 6).[18]

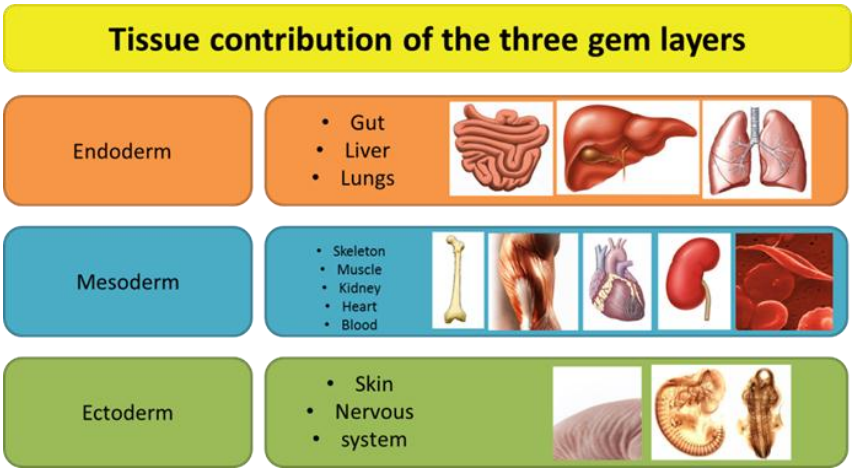

Figure 6: Tissue contribution of the three germ layers. Schematic illustration which depicts the three germ layers and respective tissues that they will become in the future.

The gastrulation begins approximately 6.5 days after fertilization where the epiblast cells lose their epithelial continuity at one point on the border of the cup and ingress to form a new tissue layer, the mesoderm (Figure 7).[18]

This site of new tissue production symbolizes the formation of the primitive streak and marks the beginning of gastrulation.[7] Along the next 12h the primitive streak elongates to reach the distal tip of the cylinder and therefore produces a line (or streak) of epiblast ingression and mesoderm production.[19] The place where the streak forms marks the posterior extreme of the embryo and the AP axis is now present, effectively running from the location where the streak formed to the distal tip of the cylinder and up to an anterior point on the other side of the border diametrically opposite the streak.[19]

The anterior extreme of the streak, that is close to the distal tip of the cylinder forms a specialized structure named the node. It is from the node that the most dorsal mesoderm in the embryo, the prechordal plate and notochord, are created. Definitive gut endoderm as well emerges from the epiblast in the vicinity of the node and intercalates into the existing visceral endoderm layer, in time fully replacing it. Together, midline mesoderm and endoderm derived from the node are known as axial mesendoderm.[11]

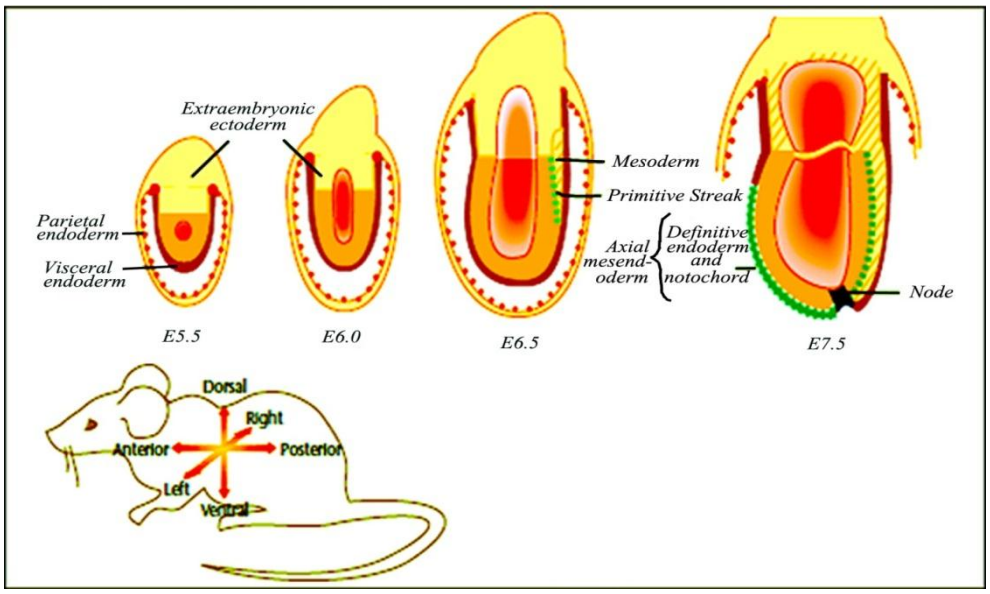

Figure 7: Development of the mouse embryo layers from fertilization to gastrulation. E 6.5, gastrulation begins and the primitive streak forms at the embryonic–extraembryonic junction. Mesoderm is produced in the streak. The origin of the streak indicates the posterior aspect of the future organism. By E7.5 the streak has elongated to the distal tip of the embryo and its anterior end has formed a specialized structure, the node. Axial mesendoderm derives from the node and moves anteriorly to underly prospective neurectoderm. The axes of the future organism are explicit at E6.5 and are revealed superimposed on an adult mouse. On the left are represented the future body axis of the mouse. (Adapted from Beddington 1999)

1.3.3 Primitive Streak

The epiblast is composed by pluripotent cells which will originate the primitive streak. The primitive streak designates the posterior end of the fetus and is created by the movement of epiblast cells inwards through a narrow band starting at the junction between the epiblast and extraembryonic ectoderm (Figure 7).[11] What initiates the

movement in this particular place is at present unclear, nevertheless doubtless expression of genes (*Lefty1* and *Cerl1* for example) producing molecular asymmetry is involved.[11]

As the streak extends anteriorly, epiblast cells translocate into it and emerge as mesoderm. After reaching the distal tip of the egg cylinder, the anterior streak condenses into the 'node', and afterwards elongates anteriorly to form the notochord.[20] The length of the streak characterizes the extent of gastrulation and, since it is difficult to detect grossly, expression of Brachyury (T), a DNA-binding protein, is frequently used. Brachyury is thought to be related whit the migration of nascent mesoderm out of the streak.[20]

1.3.4 The Node

The node is a restricted area of the primitive streak which will give rise to the notochord and consequently has a vital role to play in patterning the midline axis of the mouse embryo.[21] It seems like a discrete morphological structure in the ventral midline at the rostral end of the late primitive streak at about E7.5.[21]

The concept of the organizer began with the finding of the induction in the eye and eventually increased into a unifying concept of early organization of the embryo with the classic studies of H. Spemann and H. Mangold in the 1920s, where transplantation of a small piece of non-pigmented dorsal region of a donor newt embryo to the ventral side of a pigmented host embryo caused the induction and recruitment of host cells to form a secondary axis consisting of the neural tube, notochord and somites.[1, 8]

In mice, the anterior tip of the primitive streak condenses into the node, or 'organizer'.[22] The node forms axial mesendoderm, that includes mesoderm which will populate the midline of the embryo and the definitive gut endoderm [22] [23]. The function of the node in organizing the anterior half of the mouse embryo is an area of intense research [22, 23]. Nevertheless, its relevance as the anterior organizer has

lately been challenged by the anterior visceral endoderm (AVE), which exerts its activity in head specification earlier than the formation of the node [24, 25].

1.3.5 Anterior Visceral Endoderm (AVE)

The mammalian embryo seems to have two signaling centers: one in the node, as previously mentioned, and one in the anterior visceral endoderm (AVE).[11]

A growing number of genes have been identified that are expressed in anterior visceral endoderm (AVE) prior or coincident with, the beginning of gastrulation in the mouse embryo.[23]

Though the first morphological signal of A-P asymmetry shows only with the appearance of the primitive streak at E6.5, evidence of a pre-existing molecular asymmetry in the visceral endoderm (VE), is already present at E5.5. The first sign of the existence of molecular asymmetry in the visceral endoderm derived from the expression of the VE-1 antigen, that is expressed in the anterior region of the visceral endoderm.[26] Expression of the VE-1 antigen4 and Otx2 [27, 28], Lim1 [25], goosecoid (gsc)[25], Hex[29] and cerberus-like 1 [25] genes in the AVE evidently precedes the beginning of gastrulation by half a day or more. They all seem to be co-expressed in a medial strip of visceral endoderm underlying almost the anterior third of the embryo, and their expression prior primitive-streak formation makes it impossible that localization of their transcripts is influenced by products of the streak.[11] Consequently, this strip of visceral endoderm is additionally patterned, being subdivided at the time of primitive-streak formation into at least two distinct domains.[11] The most anterior domain that corresponds to the site of future heart development, is evidenced by the beginning of Mrg1 expression.[30] Subsequently, Hesx1 is expressed in a population of AVE that overlies epiblast fated to form anterior CNS.[29] The expression of Mrg1 and Hesx1 in the AVE, while coincident with the onset of gastrulation, is as well improbable to be influenced by products of the primitive streak because their transcripts are sensed on the opposite side of the egg cylinder from the nascent streak, being disconnected from it by the proamniotic cavity.[30]

Consequently, molecular description shows that the AVE has a single identity at least a day before overt gastrulation starts and that it obtains more complex pattern prior any interaction may have happened with mesoderm or endoderm produced during gastrulation.[11, 31]

The AVE is originated from the visceral endoderm (hypoblast) that migrates forward. As this region migrates, two antagonists of the Nodal protein are secreted, Lefty1 and Cerberus.[31] Lefty1 binds to the Nodal's receptors and inhibits Nodal

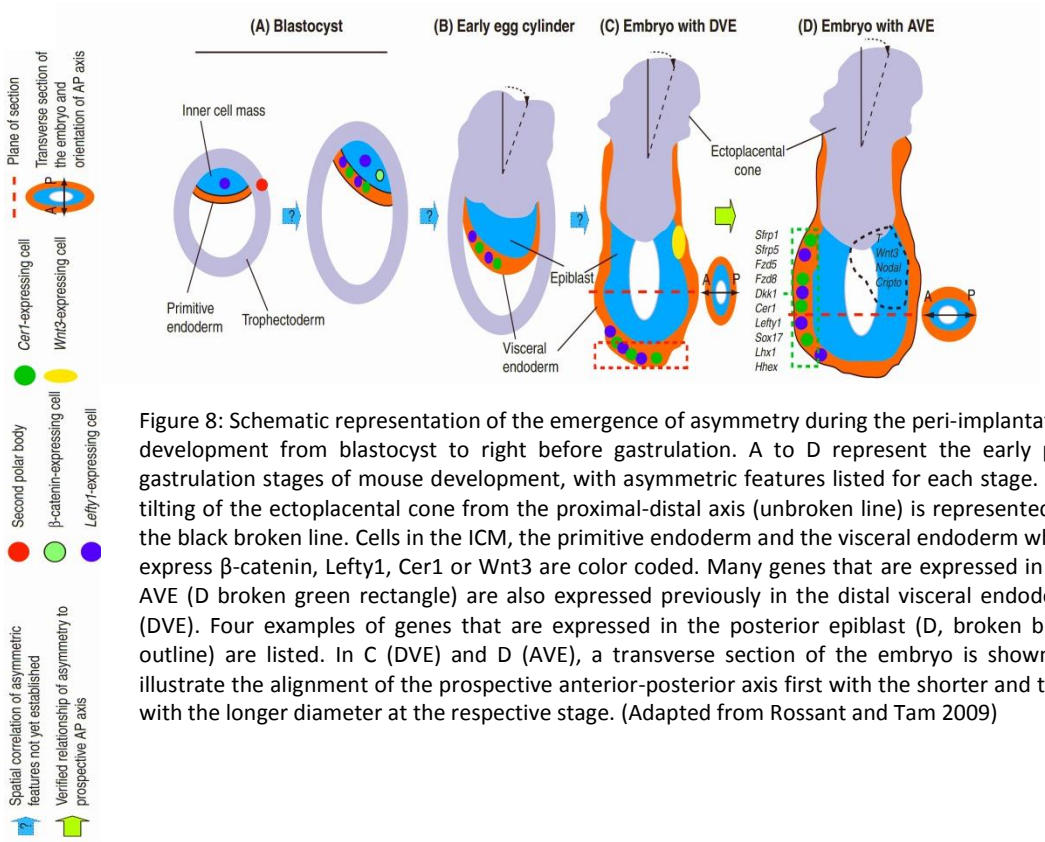

Figure 8: Schematic representation of the emergence of asymmetry during the peri-implantation development from blastocyst to right before gastrulation. A to D represent the early pre-gastrulation stages of mouse development, with asymmetric features listed for each stage. The tilting of the ectoplacental cone from the proximal-distal axis (unbroken line) is represented by the black broken line. Cells in the ICM, the primitive endoderm and the visceral endoderm which express β-catenin, Lefty1, Cer1 or Wnt3 are color coded. Many genes that are expressed in the AVE (D broken green rectangle) are also expressed previously in the distal visceral endoderm (DVE). Four examples of genes that are expressed in the posterior epiblast (D, broken black outline) are listed. In C (DVE) and D (AVE), a transverse section of the embryo is shown to illustrate the alignment of the prospective anterior-posterior axis first with the shorter and then with the longer diameter at the respective stage. (Adapted from Rossant and Tam 2009)

binding, and Cerberus binds to Nodal itself. [25, 31, 32] Whereas the Nodal proteins inside the epiblast activate the expression of posterior genes that are needed for mesoderm formation, the AVE generated an anterior region where Nodal cannot act.[33] The AVE also starts expressing the anterior markers Otx2 and Wnt inhibitor Dickkopf.[34] Experiments of mutant mice indicate that the AVE induces anterior

specification by suppressing posterior patterning by Nodal and Wnt proteins.[33] Nevertheless, the AVE by itself cannot promote neural tissue, as the node can.[35]

After formation, the node will secrete Chordin; the head process and notochord will later and Noggin. These two BMP antagonists are not expressed in the AVE.[36] Whereas knockouts of both the chordin and the noggin gene do not disturb development, mice lacking both genes miss a forebrain, nose, and other facial structures.[36] It is possible that the AVE acts in the epiblast to restrict the Nodal signal, thus collaborating with the node-produced mesendoderm to induce the head-forming genes to be expressed in the anterior portion of the epiblast.[1]

1.4 Kidney Development

The intermediate mesoderm generates the urogenital system, in other words, the kidneys, the gonads, and their respective duct systems in mammalians.[37]

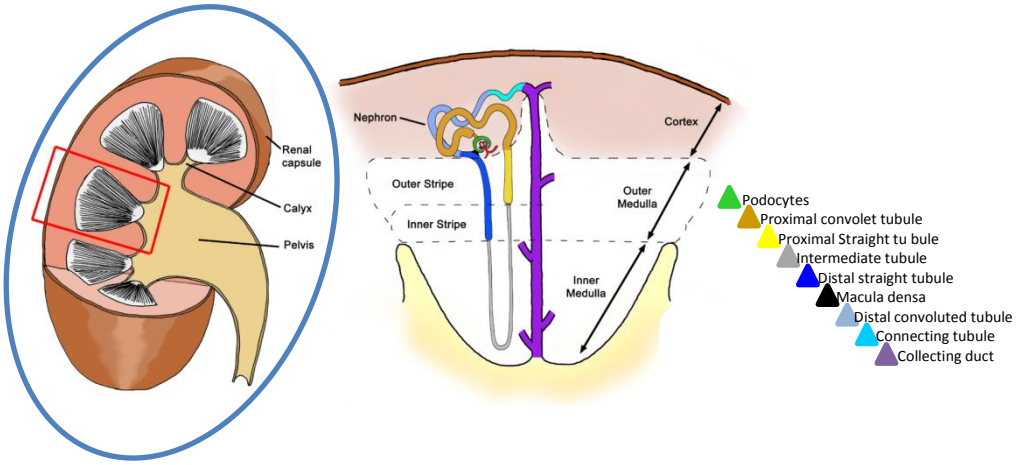

Figure 9: Illustration of the structure of the mammalian kidney. Each kidney is composed of a fibrous outer layer named the renal capsule, a peripheral layer named the cortex, and an inner layer named the medulla. The medulla is arranged in multiple pyramidal structures that together with overlying cortex comprise a renal lobe (red box). Urine drains from the tip of each pyramid (papilla) into minor and major calices which empty into the renal pelvis. The renal pelvis then transmits the urine to the bladder through the ureter. Nephrons are found within the cortex and medulla and have a characteristic structure that involves a glomerular blood filter containing podocytes and a tubular epithelium that loops down into the medulla. The tubule is subdivided into proximal, intermediate and distal segments (see color key) that are essential for the recovery and modification of the glomerular filtrate. (Adapted from Kidney of Mouse Development Stem book.org)

Mouse kidney development is also named nephrogenesis, proceeds through a series of three successive phases: the pronephros, mesonephrons and metanephros. The development starts with the formation of the pronephric duct (also known as the nephric or Wolffian duct; Figure 9). The nephric duct arises from the cranial portion of the intermediate mesoderm and grows caudally down the trunk to merge with the urogenital sinus (ventral portion of the cloaca) at E11 (Hoar, 1976). As it migrates, the nephric duct induces the generation of mesonephric nephrons from the adjacent intermediate mesoderm (known as the nephrogenic cord or nephrogenic mesenchyme).[37] Metanephros development is initiated at E10.5 at the caudal end of the nephric duct level with the hindlimb (27–28th somite).[37] Glial-derived growth factor (GDNF), secreted from a unique population of nephrogenic cells called the metanephric mesenchyme, promoves an elongates from the nephric duct named the ureteric bud (UB) that then invades the metanephric mesenchyme, giving rise to the collecting ducts, pelvis, and ureter. (see Figure 10 and 11) [37].

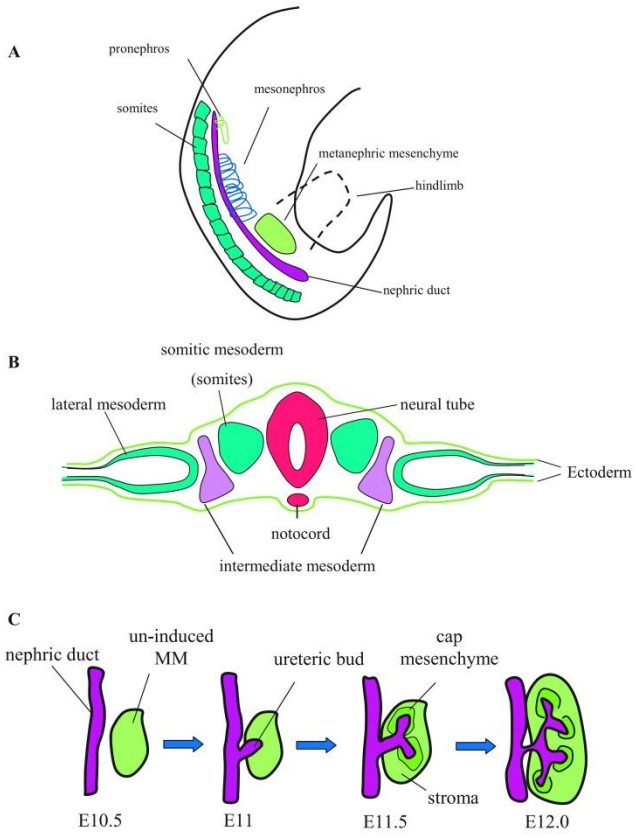

The UB origins a T-shaped bifurcation at E11.5, and then undergoes around 11 cycles of branching and elongation to generate the metanephric collecting duct system. [38]

Figure 10: Representation of the early even in mammalian kidney development. A: sagittal view of kidney components at embryonic E10.5. B: cross section of an E8.0 embryo. Nephrogenic tissues are specified from the intermediate mesoderm by signals from the surface ectoderm and somites. C: ureteric bud outgrowth and early patterning of the metanephric mesenchyme (MM). Gdnf expression by the MM promotes outgrowth and invasion of the ureteric bud at E11. Ureteric bud invasion rescues the MM from apoptosis and stimulates the condensation of the cap mesenchyme around its tip. (Adapted from Scott Boyle and Mark de Caestecker, 2006)

During this process, the UB tips are surrounded by a cap of metanephric mesenchyme, a subset of which form the nephron progenitors that proliferate, differentiate into glomerular and tubular epithelial cells, and fuse with the collecting duct. Previous studies demonstrated that reciprocal and inductive signaling between the UB and the metanephric mesenchyme are essential for starting and maintaining the cycles of UB branching and nephron induction that underlie the formation of the metanephros (Figure 11). [39] The permanent kidney of amniotes, the metanephros, is generated by some of the same components as the earlier, transient kidneys types.[40]

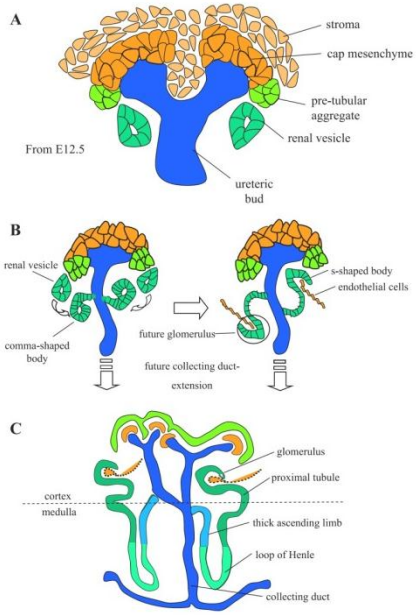

Figure 11: Schematic representation of the formation and patterning of nephrons. A: Early differentiation. The condensed cap mesenchyme becomes distinct from the surrounding stromal mesenchyme by E11.5. B: nephron elongation, fusion with the ureteric bud, and vacularization. Nephrogenesis proceeds with the formation of the comma- and S-shaped bodies and early fusion of the future distal segment with ureteric bud epithelium. Endothelial cells invade the glomerular cleft of the S-shaped body. C: patterning of nephron segments. A second temporally distinct phase of nephrogenesis occurs after E16.5 in the mouse in which there is increased growth and patterning of nephron segments associated with expansion of the renal cortex and patterning of the medullary region of the adult kidney. (Adapted from Scott Boyle and Mark de Caestecker, 2006)

1.4.1 Genes Involved in Renal Development

More than 400 genes are known to be expressed during nephrogenesis.[40] The list includes transcription factors, growth factors, signaling molecules and extracellular matrix molecules, and data on them is catalogued in the Kidney Development Database, which is kept up to date and is available online over the Internet.

Several signaling pathways are involved in kidney development. In our context the kidney and its signaling pathways are very interesting because the development of kidneys in the *Adtk1* knock-out mice (*Adtk1*$^{-/-}$) seem to be affected by the absence of this gene. In this work particular attention was given to the relationship between *Wnt4*, *Gremlin1*, *BMP4*, *C-RET* and *GDNF* genes and *Adtk1* since they are related to kidney development.

1.4.1.1 GDNF- Glial-Derived Neurotrophic Factor

Gdnf is expressed throughout the nephrogenic cord at E9.5 but turns out to be restricted to the region of the metanephric mesenchyme by E10.5. [41-43] GDNF signals over the Ret tyrosine kinase receptor, that is expressed by the nephric duct, organized with a membrane-tethered GFRa1 co-receptor. [44] [45] [46] GDNF signaling also implies cell surface heparan sulphate glycosaminoglycans that bind to GDNF and can have a role in ligand exhibition to the receptor.[47] Most of mouse embryos deficient in Gdnf, Ret, or Gfra1 fail to form a UB, even though the observation that a UB forms in a portion of the mutants shows that additional UB inducing signals must also exist. [48, 49] [50] [43] [51]

Several experiments using GDNF-soaked beads and transgenic overexpression of Gdnf have shown the importance of localizing GDNF-Ret signaling in order to prevent the formation of ectopic UBs.[52] [53] The maintenance and/or activation of Gdnf expression in the metanephric mesenchyme relay on a host of regulatory factors including transcription factors (Eya1, Six1, Sall1, Pax2, Hox11 proteins), secreted factors (Gdf11, Nephronectin) and FGF signaling. Inhibitors of Gdnf expression include

Foxc1, a forkhead transcription factor, and the Robo2/Slit2 receptor/ligand pair best known for their chemorepellent role during neuron and axon migration [54].

1.4.1.2 Ret proto-oncogene (C-RET)

Additionally to promoting UB outgrowth, GDNF-Ret signaling also has a crucial role in subsequent UB branching, most likely by stimulating the cell migration and proliferation that characterizes the UB tip [55]. After UB invasion of the metanephric mesenchyme, Gdnf turns out to be expressed in the cap mesenchyme surrounding each UB tip.[42] [53] Expression of Ret becomes restricted to the UB tips and the continuance of this expression pattern relies upon retinoic acid signaling, consistent with earlier remarks linking vitamin A/retinol deficiency with renal abnormalities. [56, 57] Looking at the expression of retinoic acid receptors, retinoic acid is not thought to signal straight to the UB nevertheless is in its place hypothesized to stimulate the discharge of an unknown Ret-inducing factor from nearby stromal cells.[56, 57] If this factor stimulates Ret expression in the UB or performs via the metanephric mesenchyme is not established. The distance of Ret to the UB tip is relevant for branching morphogenesis as miss expression of c-ret throughout the ureteric epithelia has been demonstrated to inhibit UB growth and branching in transgenic mice, probably by acting as a 'sink' for GDNF ([58]). Ret null embryos do not have defects in nephric duct extension therefore other Gata3 targets must exist.[59]

1.4.1.3 Bone Morphogenetic Protein 4 (BMP4) and Gremlin1

BMP4 is implicated as a negative regulator of UB outgrowth. It is expressed in stromal cells enveloping the nephric duct before the outgrowth of the UB [60]. Even though Bmp4 null embryos die during early development, heterozygotes commonly display an ectopic UB.[61, 62] Organ culture experiments have shown that BMP4 may block the capacity of GDNF to promote ectopic budding from the nephric duct.[52] BMP4 activity can be inhibited after binding to the secreted BMP antagonist encoded by Gremlin1 (Grem1), that is expressed in an overlapping expression domain with Bmp4 in the early stages of UB outgrowth (Hsu et al., 1998; Michos et al., 2007; Michos

et al., 2004). Grem1-deficient embryos exhibit blocked UB outgrowth and most of animals are born without metanephric kidneys. These defects are liberated after inactivation of one copy of the Bmp4 gene, consistent with the Grem1 null phenotype that is originated by excessive BMP4 signaling.[63] Expression of Gdnf in the Grem1 mutant metanephric mesenchyme is at the beginning normal but is downregulated progressively and lost by E11.75.[63] Despite the fact that these observations indicate that locally inhibiting BMP4 signaling around the nascent UB is necessary to maintain Gdnf expression, treatment of isolated metanephric mesenchyme with either BMP4 or Grem1 does not modify Gdnf expression.[63]

1.4.1.4 Wnts signaling and Wnt4

Wnt signaling via the canonical β-catenin pathway has been connected by several authors in UB branching.[64] Experiments with transgenic reporter mice have shown that β-catenin-induced genes are active in the UB during branching morphogenesis.[64] UB-specific inactivation of β-catenin stops branching at E12.5 resulting in renal aplasia or renal dysplasia.[65] Furthermore, this phenotype is related with reduced expression of Gdnf and Ret in the cap mesenchyme and UB tip, respectively. Several Wnts capable of signaling through the canonical β-catenin pathway are expressed in the developing metanephros, including Wnt6, Wnt7b, and Wnt9b in the collecting duct system, and Wnt4 in early nephron precursor.[66] Between these last ones, loss of Wnt4 or Wnt9b conducts to a disruption in UB branching following the T-stage, with the Wnt9b mutant phenotype being more aggressive than the Wnt4 mutant phenotype.[67] Verifying that a branching defect occurs after loss of Wnt4, that is expressed in the renal vesicle under the UB tip, indicates a feedback proccess in which nephrons induced in response to branching use Wnt4 to induce consequent UB branching.[67] In Wnt9b mutant embryos, expression of Wnt11 and Gdnf is downregulated before the morphological form of the branching defect.[68] Nevertheless, given the reciprocal nature of interactions happening between the cap mesenchyme and the UB tip and the presence of a GDNF-Ret auto-

regulatory loop, it is not of our knowledge if the cellular target of Wnt9b activity is the cap mesenchyme or the UB.[68]

Wnt4 is expressed by the pre-tubular aggregates and is thought to work in an autocrine way to propagate the initial Wnt signal and complete the transition to the renal vesicle stage.[67] Both Wnt9b and Wnt4 perform signal via the canonical β-catenin pathway however can use different receptors and proceed in a linear pathway as Wnt9b is incapable to promote nephrogenesis in Wnt4 mutant mesenchyme in vitro.[67, 68] Gain-of-function experiments testing the effect of sustained β-catenin signaling in the metanephric mesenchyme indicate that even though Wnt signaling is crucial during the early phases of the nephrogenic program, it has to be attenuated at later stages so that nephron progenitors undergo a mesenchymal-to-epithelial transition.[37, 69]

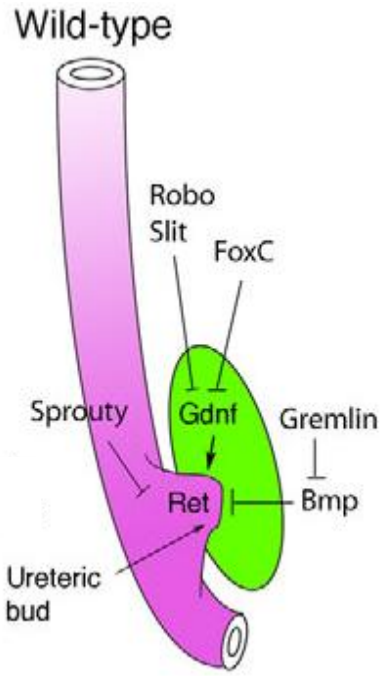

Figure 12: Schematic representation of the signals that promote or suppress the ureteric bud outgrowth. The outgrowth and invasion of the ureteric bud (UB) from the nephric duct starts the metanephric kidney development. In a wild-type embryo, the Gdnf secretion from the metanephric mesenchyme promotes the receptor tyrosine kinase Ret, via the co-receptor Gfra1 and promotes the UB outgrowth and invasion. (Adapted from Gregory R. Dressler, 2009)

1.5 Neural Tube Defects

Neural tube defects (NTDs) are congenital abnormalities of the central nervous system and axial skeleton that go from the fatal to the asymptomatic[70]. NTDs may be classified based on the embryonic event that is disturbed, and can result from a series of genetic defects and environmental influences.[70] Comprehending the genetic and embryonic basis of NTDs is showing the underlying developmental mechanisms, and allowing new approaches towards prevention of these severe birth defects.

To understand the embryonic origin of NTDs, it is needed to appreciate the normal developmental processes of (i) neurulation, by which the neural tube is composed, (ii) axial skeletogenesis, in which the skull and vertebral column differentiate and become modeled around the neural tube and (iii) tail bud development, that is responsible for formation of the entire body structure at post-lumbar levels of the body axis[70].

1.5.1Neurulation

Neurulation is the embryonic step that is responsible for the formation of the brain and spinal cord.[1] It starts with neural induction leading to the appearance of the neural plate, a condensed area of ectoderm in the dorsal midline.[1] The edges of the neural plate curve dorsally, starting at about 17–18 days post-fertilization, defining a longitudinal neural groove that expands with progressive elevation of the sides of the neural plate. The neural folds converge towards the midline and fuse, creating the neural tube.[1]

The initial closure event (Closure 1) occurs on E 8.5 in the mouse and is located at the future cervical/occipital boundary (Figure 13).[71] Fusion takes place from this level in rostral and caudal directions. Fusion is initiated separately, soon after this initial closure event, at two sites within the developing brain: Closure 2 is situated at the boundary between the midbrain and forebrain, while Closure 3 occurs at the extreme rostral end of the forebrain. Closure then continues in a bidirectional fashion,

with completion of closure at 'neuropores' in the forebrain, hindbrain and low spinal region.[71]

This multisite closure process has been defined mainly in mouse embryos and was extrapolated to occur also in human development, on the basis of interpretation of NTD patterns in late fetuses.[72] Looking closer, mouse Closure 2 is currently recognized to be variable in its axial level among different genetic strains.[4] Consequently, Closure 2, even in the mouse, is not mandatory for brain formation. In contrast, Closure sites 1 and 3 are crucial for well succeeded neural tube closure.[72] Embryos in which Closure 1 fails develop craniorachischisis, where the neural tube is open from midbrain to low spine, while failure of Closure 3 leads to anencephaly with split face.[72] An aim for future investigation will be to determine the genetic variances that control the axial level of Closure 2, and to study if such genetic factors might explain the differing incidence of cranial NTDs.[72]

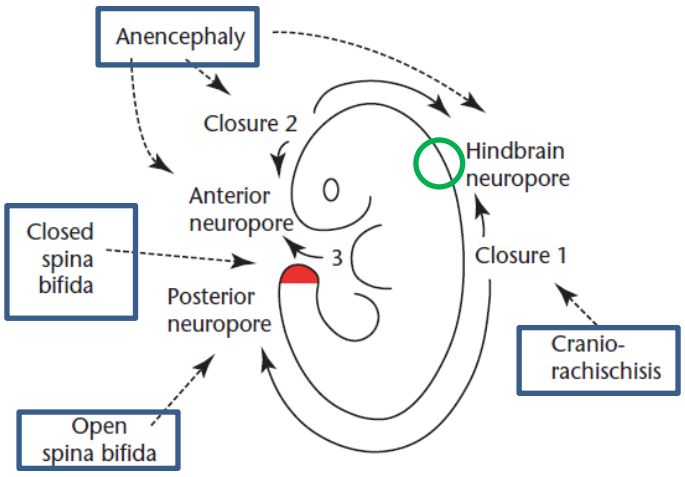

Figure 13: Multisite closure of the neural tube in the mouse embryo. Schematic summary of the successive initiation events of mouse neurulation (Closures 1, 2 and 3), the direction of spread of closure from the initiation sites (solid arrows) and the sites of completion of closure (anterior, hindbrain and posterior neuropores). The tail bud region (red shading) is the site of secondary neurulation which follows immediately after closure of the posterior neuropore. The main types of neural tube defect that result from failure of the different components of neurulation are indicated by the dotted arrows. Adapted from Copp AJ and Bernfield M (1994) Etiology and pathogenesis of human neural tube defects: Insights from mouse models. Current Opinion Pediatrics 6, 624–631.

At E10.5 in mice, occurs the closure of the posterior neuropore in the upper sacral region, which marks the end of primary neurulation. Formation of the neural tube in the lower sacral and caudal regions happens by a different process that involves canalization of a solid cord of cells during tail bud development, without the closure of neural folds (secondary neurulation).[1]

1.5.2 Axial Skeletogenesis

After the gastrulation, the paraxial mesoderm flanking the closing occipital and spinal neural tube comes to be subdivided to form the segmentally organized, epithelial somites.[19] Both somites differentiate by the breakdown of their ventromedial wall to form the sclerotome, while their dorsolateral wall continues epithelial, comprising the dermomyotome.[8] Afterwards the dermomyotome undergoes an epithelio-mesenchymal transformation with cells delaminating from its dorsal and ventral edges to form the myotome. Axial skeletal development starts when the sclerotomal component of the mesodermal somites migrates to encompass the freshly closed neural tube, subsequently undergoing cartilaginous and bony differentiation to create the entire vertebrae.[73]

By contrast to spinal levels, in the cranial region, the skeletal structures are not formed completely from mesoderm. Fate mapping studies in birds first demonstrated that considerable portions of the skull and facial skeleton are resultant from cells of the neural crest, while related experiments in mouse reveal a larger contribution by the cranial mesoderm to the mammalian skull [74]. However, it is commonly agreed that the cranial skeleton of higher vertebrates is a composite of both mesoderm- and neural crest-derived cells.[73]

Closure of the cranial neural tube is crucial not only to main the brain development, but also for the formation of the skull vault. The embryonic brain works as a physical ‘template’ over which the skull becomes modeled. The absence of cranial neural tube closure, as in anencephaly, leads certainly to failure of formation of the skull vault, while the skull base is always present although invariably deformed. Later,

both neural and skeletal development is contingent upon normal closure of the cranial neural tube, although for different motives.[75]

1.5.3 Tail Bud Development

The tail bud represents, at the lowest spinal levels, the remnant of the primitive streak and is the fundamental source of all nonepidermal tissues including the neural tube (via secondary neurulation) and the vertebrae.[1] The tail bud comprises a self-renewing stem cell population whose derivatives proliferate quickly leading to longitudinal growth of the body axis.[11] As cells remain in the wake of the 'retreating' tail bud, condense into cell masses that afterwards differentiate to form the most important structures of the post-lumbar region: the neural tube, notochord, somites and hindgut.[1] The neural tube is created when this cellular condensation forms a neuroepitheliumin a process named 'canalization', by which the solid neural precursor is transformed to a hollow secondary neural tube.[7] Cell lineage analysis show that tissues of the low body axis come from the same stem cell population, opposite to the corresponding tissues at higher levels of the body axis that arise from different 'germ layers' of the gastrulation stage embryo.[11]

1.5.4 Genes involved in Developmental Mechanisms of Neural

1.5.4.1Tube Defects

For successful neurulation in mice more than 190 genes are needed, with NTDs arising in embryos missing function of any one of these genes. Furthermore, a great number of nongenetic factors (e.g. drugs, metabolites, physical factors) may cause NTDs in animal experiments.[71] The developmental basis of three distinct events of neurulation has received particular consideration in the late years: (i) the genetic and cellular events required for the first closure event (Closure 1), whose failure leads to craniorachischisis; (ii) the molecular signalling interactions which govern bending of the neural plate during closure of the spinal neural tube, whose failure leads to

myelomeningocele (open spina bifida); (iii) the vast and complex genetic and cellular events that are essential for cranial neural tube closure, whose failure leads to anencephaly.[1]

1.5.4.2 Role of Planar Cell Polarity (PCP) signalling in the initiation of Neurulation

When the initial closure event, Closure 1, fails it results in the development of craniorachischisis, in which the embryo has a widely open neural tube, from midbrain to low spine.[71] Lately, it has become clear that embryonic shaping is a requirement for successful Closure 1. The vertebrate embryo experiences extensive shaping during the late stages of gastrulation, as the elliptical gastrula is transformed into the keyhole-shaped neurula.[71] This shaping is caused largely by the cell movements of convergent extension which involve lateral to medial displacement of cells in the plane of the ectoderm, and in the underlying mesoderm. Cell intercalation in the midline conducts to rostrocaudal extension of the body axis.[8]

A crucial role in convergent extension has been attributed to the planar cell polarity (PCP) pathway, an extremely conserved, noncanonical Wnt/frizzled/ dishevelled intracellular signalling cascade. Initially described in the fruit fly, Drosophila, PCP signalling is nowadays known to play a key role in creating and keeping the polarity in several epithelial and nonepithelial vertebrate tissues. The first signs to a role for PCP signalling in neurulation derived from experiments with the frog, *Xenopus leavis*. The incorrect expression of PCP pathway proteins inhibited convergent extension, and produced embryos with an abnormally short, broad neural plate that failed to complete neural tube closure [76]

The flaws in *Xenopus leavis* closely resemble the NTDs in mouse embryos lacking function of numerous genes of the PCP pathway, including Vangl2,[77] [78] Scrb1 and Celsr1.[79] Analogous flaws are seen in mice lacking function of two dishevelled genes or two frizzled genes.[80] In all of these mouse mutants, the neural plate is abnormally broad and has a nonbending region prevailing between the neural

folds, opposite to the well-defined midline bending point of normal embryos. Though the neural folds rise apparently normally, they are situated too far apart to accomplish closure (Figure 4).[71] Recent studies have showed that convergent extension movements are defective in Vangl2 mutant mouse embryos, just before failure of Closure 1, validating the relation between PCP signalling, convergent extension and initiation of neural tube closure in mammals.[81] A significant aim for this study is to determine if the defects in PCP signaling can also underlie cases of craniorachischisis in humans, as well as in mice.

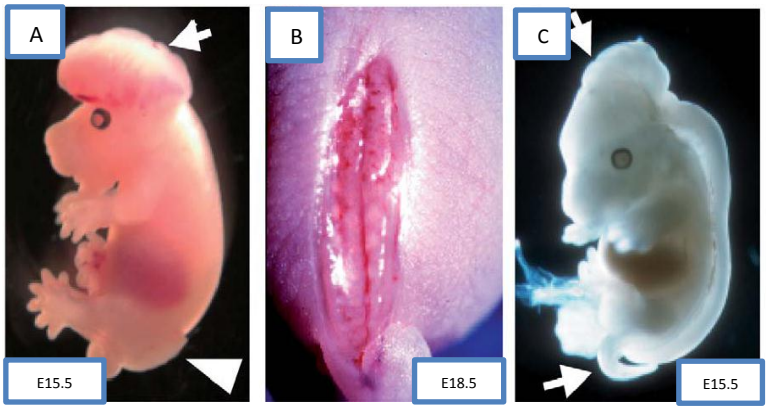

Figure 14: Mouse neural tube defects. A - exencephaly (arrow) and open spina bifida (arrowhead) in E15.5 mouse embryo homozygous for the curly tail mutation; B open spina bifida at E18.5 in Vangl2 double mutant mouse fetus. C- craniorachischisis in at E15.5 in double mutant mouse for Celsr1. Adapted from Copp AJ, Greene NDE and Murdoch JN (2003) The genetic basis of mammalian neurulation. Nature Reviews. Genetics 4, 784–793;

1.5.4.3 Regulation of Neural Plate Bending: Mechanisms of Spina Bifida

Closure 1 involves bending of the neural plate solely in the midline (at the median hinge point), but closure of the neural tube at low spinal levels furthermore involves bending at paired dorsolateral hinge points, located close to the location at which neural plate and surface ectoderm first separate from each other (Figure 16). If dorsolateral hinge point formation fails, as in the Zic2 mutant mouse [81], the neural tube stays open and spina bifida (myelomeningocele) occurs. It is essential, therefore, to comprehend the molecular mechanisms by which dorsolateral hinge point formation is controlled.[81]

Dorsoventral molecular interactions are recognized to regulate the pattern of neuronal and glial differentiation in the post-closure neural tube.[7] Recently, it has been verified that similar interactions operate earlier in development, to establish the cellular behaviour of the bending neural plate. Whereas signals from the notochord, including Shh, are needed to induce midline bending, the neural tube may still close even in the absence of a notochord. This indicates the existence of a 'default' mechanism of neural tube closure that functions in the absence of Shh influence. A reason for this observation has come from studies in which the neural folds of cultured mouse embryos were implanted with beads soaked in diffusible signalling molecules throughout spinal neurulation.[82]

BMP2 is a signalling molecule that is generally secreted from the dorsal-most surface ectoderm, covering the region where dorsolateral hinge points form, in contrast to Shh that is produced ventrally, from the notochord. Exposure of a neural fold to both BMP2 and Shh peptides seems to inhibit dorsolateral hinge point formation.[81] Furthermore, mice lacking BMP2 or Shh function both display premature, extravagant dorsolateral hinge points. Consequently, both dorsal BMP2 and ventral Shh are inhibitory to dorsolateral bending. For a dorsolateral hinge point to form, therefore, the influence of both BMP and Shh must be decreased. For BMP, this is accomplished via secretion of Noggin, a BMP antagonist, from the dorsal-most neural plate cells.[81] Using Noggin from an implanted bead, even in the presence of BMP2, was found to promote a dorsolateral bend. Shh inhibits Noggin production, clarifying the inhibitory effect of strong Shh signalling on DLHPs in the upper spine. Nevertheless, as the wave of spinal neurulation passes down the body axis, the st rength of Shh signalling lessens, allowing Noggin to be secreted and dorsolateral hinge points to 'break through', at lower spinal levels. For this reason, a complex set of molecular interactions (Figure 15) regulates dorsolateral neural plate bending in the low spine, just before to completion of primary neurulation.[71, 81]

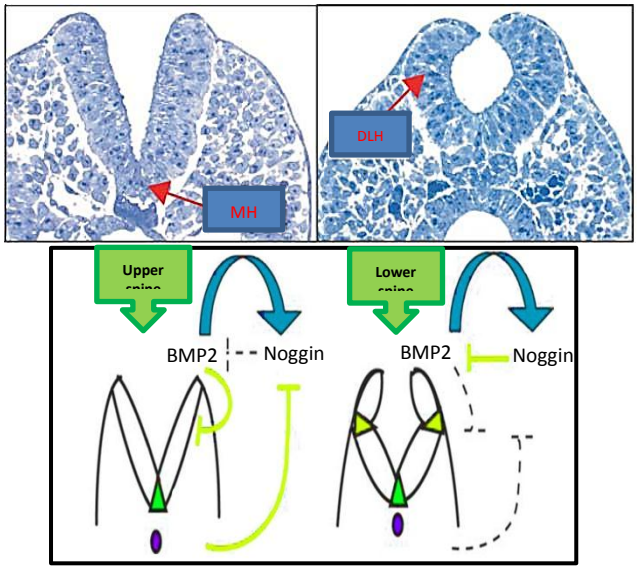

Figure 15: Molecular regulation of dorsolateral bending in mice neural tube closure. The morphology of neural tube closure modifies from (A) high spinal to (B) low spinal areas of the mouse embryo. In the upper spine, the neural plate bends only in the midline, at the median hinge point (MHP), while in the low spine bending happens at dorsolateral hinge points (DLHPs). (C) Resume of the molecular interactions regulating DLHP formation. In the upper spine, DLHPs are absent because of unopposed inhibition by BMP2. Though transcription of Noggin is stimulated by BMP2 at all levels of the body axis, Shh expression from the notochord is high in the upper spine, blocking Noggin expression. In the lower spine, Shh effect is reduced, Noggin expression is deinhibited and antagonizes the inhibitory influence of BMP2, allowing DLHPs to form. Green triangles: MHP; limon green triangles: DLHPs; blue arrows: stimulatory interactions; limon green lines: inhibitory interactions and dashed lines: inactive influences. Adapted from Ybot-Gonzalez et al. (2007).

1.5.4.4 Molecular and cellular regulation of cranial neural tube closure

Cranial closure is more vulnerable to disturbance than spinal closure in the mouse, as demonstrated by the enlarged incidence of exencephaly (open brain) compared with spina bifida among knockouts and mutants with NTD phenotypes. Likewise, teratogenic agents stimulate mouse cranial NTDs much more commonly than spinal defects. The presence of so many mouse genetic and nongenetic models with exencephaly indicates that several different types of developmental disturbance can lead to the faulty cranial neural fold closure.[71] While exencephaly in the Twist and Cart1 knockouts has been proposed to involve defective initial expansion of the cranial neural folds, the phase of cranial neurulation that appears most often disturbed in gene knockouts is the establishment of dorsolateral bending points, without which midline neural fusion cannot happen.[83]

1.5.4.5 Neural crest emigration

The changing from biconvex to biconcave neural plate morphology can also relay on the initiation of cranial neural crest migration. In the midbrain and hindbrain, neural crest cells disconnect from the apices of the neural folds and beggin migration prior to neural tube closure, while in the spinal region neural crest emigration follows neural tube closure.[75] Mice with loss of function of the Cited2, Pax3 and Twist genes all display cranial neural crest defects and exencephaly.[84] Likewise, mice overexpressing connexin 43 and rat embryos treated in culture with chondroitinase ABC, to digest pre-existing chondroitin sulfate, show equivalent delay in neural crest emigration and dorsolateral bending of the cranial neural folds. These discoveries indicate that neural crest emigration can be essential for closure of the cranial neural tube. Nevertheless, the converse is definitely not true: cranial neural tube closure is not necessary for normal migration of the neural crest, as demonstrated by the numerous exencephalic mutants in which neural crest migration is normal.[75]

Exactly how emigration of the cranial neural crest could permit dorsolateral bending of the neural fold tips is uncertain. A decrease in cell density at this location, as the neural crest cells precede, could have a permissive role by raising the mechanical flexibility of the dorsolateral neuroepithelium. Otherwise, abnormal retention of the apparent neural crest cells might offer a more precise inhibitory effect on the cellular mechanism of dorsolateral bending in the neural plate.[85]

1.6 The *Adtk1* (Anterior Distal Tyrosine Kinase 1) Gene

Several signaling pathways that are present in the different stages and structures of embryonic development are already known. However, several key genes that may be regulating some signaling pathways, or making the bridge between different signaling pathways, remain to be discovered.

In order to gain a better understanding of the mechanisms required for primary induction of anterior neural structures, a differential screening, using GeneChip® Arrays (Affymetrix®), was performed and several novel genes were identified with expression in the anterior distal (Ad) region (AVE and underlying ectoderm.[86] One of the 288 identified genes was *Adtk1* (*Anterior Distal Tyrosine Kinase*) which was showed an up regulation of 5.68-fold change in the anterior distal part of the AVE in mouse embryos. [86] *Adtk1* encodes for a 493 amino acid (aa) protein with a genomic distribution consisting of seven exons, and contain a predicted Ser/Thr/Tyr kinase catalytic domain.[86] This type of proteins are known to play essential roles in embryonic development through phosphorylation of key substrates such as Nodal and Wnt signaling pathways .[33, 87] However, the putative catalytic domain of *Adtk1* may be inactive as some of the catalytic consensus sites required for its function were not detected in this protein. Nevertheless, previous studies have demonstrated that defective or inactive kinases play important roles in vertebrate development.[88, 89] A defective kinase very similar to *Adtk1* is PTK7 that has been reported to be involved in Planar Cell Polarity (PCP) signaling pathway and to be essential for correct neural tube closure.[89, 90]

Comparison of the sequences of Adtk1 protein between different species reveals that mouse *Adtk1* shares 92% of identity with human ADTK1, 60 and 42% with *Xenopus Adtk1* and *Xenopus Adtk2*, 37% identity with chicken *Adtk1* and 28% identity with chicken *Adtk2* (see Table 1). [86]

It is interesting how mouse *Adtk1* sequence resembles the human one, being so different from *Xenopus* and chicken. However, it is important to remember, that both

Xenopus and chicken have two orthologs for the same gene, and only one gene exists in human and mouse. [86] Moreover, data from the expression pattern of *Adtk1* orthologs, performed in *Xenopus* and chicken, indicates that overlapping the expression patterns of the two orthologs, it resembles mouse the expression pattern (Vitorino, M unpublished).[91]

In order to assess the role of *Adtk1* in mouse embryonic development, knockout mice have been generated, by our group and others, through targeted inactivation. [86, 92] [93]Reported phenotypic analysis has shown that *Adtk1* knockout mice present several abnormalities related with bone morphogenesis and differentiation and also development of other organs as lungs, intestines. [86] [92, 93] Recently, we have determined that *Adtk1* is expressed in mouse kidneys during embryonic development (from E12.5 up to birth). Nevertheless, further studies are needed to understand the role of *Adtk1* in kidney development.

hAdtk1	92%				
XAdtk1	60%	62%			
XAdtk2	42%	42%	41%		
cAdtk1	37%	37%	38%	30%	
cAdtk2	28%	29%	30%	37%	29%
	mAdtk1	*hAdtk1*	*XAdtk1*	*XAdtk2*	*cAdtk1*

Table1: Sequence comparison between homolougous *Adtk1* genes. The numbe represent the percentage of homology in diferente species. m-*Mus musculus*; h-*Homo Sapiens*; X-*Xenopus leavis*; c-*Gallus gallus.*

1.7 Aim of this Project

The purpose of this project is to better understand the requirement of *Adtk1* during mouse development. More precisely, to study the molecular mechanisms involving *Adtk1* with detailed analysis of the developmental defects related with abnormal kidney development and impaired neural tube closure. Indeed, previous reports failed to detect defects at the level of the kidneys and neural tube being therefore imperative a comprehensive study of the role of *Adtk1* in these processes.

2 Material and Methods

2.1 Strains, Embryos and Staging

2.1.1 Mice

In this work, wilt-type *mus musculus* from strain C57/Bl6 were used, as well as the heterozygous mice *Adtk1* C57Bl6, generated in Gonçalves, et al (2011). The mice were kept on a C57Bl6, C57Bl6/DBA and C57Bl6/Sv129 genetic background. The animals were maintained under a controlled cycle of 12h with light and 12h without light. Males and females bred overnight and females were checked for vaginal plug during the following morning. Twelve p.m. of the day in which the plug was found was considered to be embryonic day 0.5 (E 0.5). Embryos were collected from pregnant mothers according to the desired developmental stage. The deciduas were removed (see section 2.1.2) in cold 1X Phosphate Buffer Saline (PBS)-DEPC, embryos were fixed overnight (ON) in fresh and filtered 4% Paraformaldehyde (PFA) with PBS-DEPC, and dehydrated in methanol:PBSw (1XPBS; 0,1%Tween-20) series until 100% methanol and stored at -20ºC. Embryos between E 7.5 and E8.25 were staged according to the number of somites. However, embryos between gestational day 8.5 and 13.5 were subsequently staged more carefully on the basis of morphology and specific characteristics of the organogenesis.

2.1.2 Opening the abdominal cavity and locating Female Reprodutive Organs

Mice were placed on the top of the cage with the respective tails pulled back. The neck was broken by apllying firm pressure at the base of the skull with the help of a forcep. The CO_2 inhalation method was also used when necessary. Then the animal was laid on its back on absorbent paper and soaked thoroughly in 70% ethanol from a squeeze bottle. This important step reduces the risk of contaminating the dissection

with mouse hair. The skin was pinched and a small lateral incision was performed at the midline with regular surgical scissors. Holding the skin firmly above and below the incision, the skin was pulled toward the head and tail until the abdomen was completely exposed and the fur was out of the way. Using forceps and fine scissors, the peritoneum was cut as shown. The coils of gut were pushed out of the way and the two horns of the uterus, the oviducts, and the ovaries were located and the reproductive tract was removed. The ovidut and attached segment of uterus was placed on fresh PBS1X.

2.1.3 Newborns Kidney Achievement

The newborns of the heterozygous *Adtk1* were collected form the box right after birth. Subsequently, they were anesthetized with CO_2 and placed on ice until death. Next the newborns were numerated and genotyped through polymerase chain reaction (PCR). After the genotyping results the kidneys were collected and they were analyzed and each phenotype identified and grouped study. In particular the KO kidneys were carefully removed and fixed in 4% PFA/PBS 1X for posterior histological analyses.

2.1.4 Generation of other Background Mice

Adtk1 heterozygous males were crossed with DBA and 129sv females resulting in some cases in *Adtk1* heterozygous after genotyping. When adults, these heterozygous mice for hybrid background were crossed and their newborns were collected for further analyses.

2.1.5 Preparation of Embryos and Kidneys

At several stages of mouse embryonic development, embryos and kidneys were dissected in cold PBS DEPC. They were transferred after dissected to a glass vial containing 4% paraformaldehyde (freshly made in PBSw DEPC) and left to fix overnight

at 4ºC. The next day, embryos were washed two times with PBSw DEPC. Then they were dehydrated with methanol series (25%, 50%, 75% in PBSw, 100%). Methanol 100% solution was changed two times and then the embryos were stored at -20°C.

2.2 Genotyping

For genotyping purposes, DNA was extracted from tail biopsies of young, adult and newborn mice and from the extraembryonic membranes of E8.5 and older embryos. After DNA acquisition the genotyping was determined by PCR according to the conditions that will be described in section 2.2.4.

2.2.1 DNA extraction from the tail

About 0,5cm of the tail of mice between 11-15 days of age were cut into eppendorfs and posteriorly were incubated overnight in 375 µl of tail buffer and 9 µl proteinase K (Boheringer®) from a stock of pK at 20mg/ml were added and left O/N at 55^{o}C, in a water bath.

On the following day, the tubes were removed from the bath and mixed for 5 min in the shaker at 55^{o}C. Then 125µl of a saturated NaCl solution was added and left to mix for 10 min. Then the tubes were centrifuged during 10 min at 13200 rpm. The upper phase was replaced into a new tube and 375 µl of isopropanol were added. The eppendorfs were spinned for 5 min at 13200 rpm and the supernatant was discharged. At this point a pellet could be seen at the bottom of the tube. The DNA was wash with 375µl of 70% ethanol, and centrifuged for 5 min at 13200 rpm. The supernatant was discharged and the pellet was left to dry at RT. The DNA was subsequently ressuspended in 125 µl of TE, at 37^{o}C.

2.2.2 DNA extraction from mouse embryos or extraembryonic membranes

After dissection, in the case of extraembryonic membranes or after *in situ* hybridization, embryos or parts of them were washed 3 times in PBS and were put each inside a 1,5ml tube. PBS was discharged with 1ml syringe with needle under the stereoscope, and the biological material was incubated in 37,5 µl embryo buffer with x µl pK (the composition of embryo buffer is equal to tail buffer) O/N at 55ºC.

On the following day, the tubes were removed from the bath and mixed for 5 min in the shaker at 55ºC. Then 12,5µl of a saturated NaCl solution was added and left to mix for 10 min. Then the tubes were centrifuged during 10 min at 13200 rpm. The top phase was replaced into a new tube and 37,5 µl of isopropanol was added and then mixed for about 5 min in the shaker. The eppendorfs were spinned for 5 min at 13200 rpm and the supernatant was discharged. At this point a pellet could be seen at the bottom of the tube. The DNA was wash with 37,5µl of 70% ethanol, and centrifuged for 5 min at 13200 rpm. The supernatant was discharged and the pellet was left to dry at RT. The DNA was subsequently ressuspended in 12,5 µl of TE, at RT with low agitation at 37ºC. At this point the samples are ready for genotyping through PCR.

2.2.3 Design of oligonucleotide primers for genotyping

For the design of the primers several issues were considered: the primer complementary region to the template should have around 18-25 nucleotides; the C+G content should be between 40% and 60% with an equal distribution of all four bases along the primer; internal secondary structure should be very small; the primers should not be complementary to each other at the 3' end to prevent the formation of primer dimmers; the annealing temperature is generally carried out 3-5°C lower than the calculated melting temperature Tm (in °C) = 2(A+T) + 4(G+C) at which the oligonucleotide primers dissociate from their templates (Sambrook, 2000). These properties guarantee that the amplified product will be well denatured during each

cycle of PCR. The constructed primers to test each marker are shown in the following table 1.

Tabela 1 – List of primers used for genotyping.

Primer name	Primer Sequence	Fragment size (bp)	Temperature of annealing (Cº)
Adtk1 wt Fw	CACCGACTACACCTACAAC	Wt:wt fw-wt rev 864bp Null neo fw-wt rev 544 bp	64
Adtk1 wt Rev	ACCACCACCAGGAAGCATGC		
Adtk1 neo Fw	CTCGACTGTGCCTTCTAGTT		

2.2.4 Polymerase Chain Reaction (PCR)

Taq DNA polymerase was the standard used enzyme for the amplification. The PCR reaction was performed in a sterile 0.5ml microcentrifuge tube using 2.5µL of 10x Polymerase buffer, 2.5µL 2mM solution of dNTPs, 1µL 20µM working aliquot of to each primer, 1µL 25µM of MgCl2, 5units/µL of Taq Dna polymerase, 1µL of template DNA and in a final volume of 25µL, diluted in nuclease free water. Each set of PCR included a negative control in order to detect contamination.

The amplification of DNA fragments was done by performing one first cycle of PCR at 95^{o}C for 5minutes. The samples were then subjected to 30cycles of amplification, each cycle with denaturation at 95^{o}C for 1min, annealing of the primers for 1 min in specific temperature (64^{o}C), followed by elongation at 72^{o}C for 1 min. After these 30 cycles it was performed a termination step at 72^{o}C for 10min and the samples were kept at 12^{o}C until further analyses. The PCR products were identified by electrophoresis through a 1% agarose gel in 1xTAE and stained with ethidium bromide, using markers of suitable size. The gel image was acquired with the Gene Flash Imaging System® (see following section).

2.3 Agarose gel electrophoresis for DNA and RNA

Agarose gels electrophoresis is commonly used for separating and analyzing DNA and RNA, since these fragments are separated according to their molecular weight. This technique was used to analyze RNA quality, the completion of a restriction enzyme digestion or to determine the yield of the plasmid DNA purification. The running of DNA and RNA fragments was performed in a horizontal configuration with an electric field of constant strength and direction. The agarose gels were prepared at an appropriated concentration 1-2% (w/v), in electrophoresis buffer (1xTAE or 0,5xTBE) (see appendix). The solution was heated in a microwave oven until the agarose was dissolved. Ethidium bromide was then added and poured into the mold, allowing the gel to set and solidify completely at room temperature. The gel was placed in the electrophoresis tank, and running buffer was added to cover the gel. The samples were mixed with 0,2 volume of the loading buffer (orange G 6X, see appendix) and were then loaded on the gel, as well as the size standards (1Kb) into slots on the left side of the gel (1KB Plus, see appendix). The lid of the gel was closed and the electrical leads were attached so that the DNA or RNA migrated toward the positive anode. A voltage was applied of 1-5 V/cm. When the samples or dyes migrated a sufficient distance through the gel, the electric current was turned off and the leads removed. The EtBr is a fluorescent dye that intercalates between the bases of the DNA and RNA, allowing the gel to be visualized by UV illumination. The gel was then visualized in a transilluminator (Gene Flash Imaging System®), by transmitted UV light at 302nm, and a picture was taken.

2.4 *In Situ* Hybridization (Whole Mount In Situ Hybridization-WISH)

The *in situ* hybridization technique allows specific nucleic acid sequences to be detected in embryonic tissues or sections and is widely used in Developmental Biology studies. In this study, whole mount in situ hybridization (WISH; Belo, et al. 2000) was carried out in order to detect mRNA transcripts within mice embryos. WISH comprises

several steps: 1) preparation of the anti-sense mRNA probe; 2) fixation of the embryonic material; 3) prehybridization; 4) hybridization with the specific probe; 5) immunological reaction; 6) detection.

2.4.1 Preparation of the anti-sense mRNA probe

Antisense probes were prepared according to the protocol described in Belo et al. (1997).

2.4.1.1 Transformation of Competent *E. coli*

The transformed DNA was added (no more 50ng in a volume of 10µL or less) to 50µL of competent cells (TOP10) in an eppendorf tube, under a flame of a Bunsen burner. The tube was gently shaken in order to mix their content, and stored on ice for 30 min. The tube was placed in a preheated 42ºC water bath for 90 seconds, without shaking, and rapidly transferred to an ice bath, allowing the cells to cool for 2 min. After this period, 500µL of LB medium was added and the tube was transferred to a shaking incubator set at 37ºC for 45 min to allow the bacteria to recover and to express the antibiotic resistance marker encoded by the plasmid. Appropriated volume (normally 50µL) of the transformed competent cells was transferred onto an agar plate with ampicillin and it is spread with an L shaped haunch. The plate was stored at room temperature until the liquid was absorbed, and then inverted and incubated at 37ºC for 12-14 hours.

2.4.1.2Plasmid Amplification

A single colony of transformed bacteria was collected using a micropipette tip and inoculated overnight on a 15mL plastic falcon tube containing 3mL of liquid LB medium with 100µL/mL of ampicillin at 37ºC and in a shaking incubator. Bacteria were harvested by centrifuging at 5000g during 30 minutes at 4ºC.

2.4.1.3 Plasmid DNA Isolation and Purification

The QIAprep mini prep procedure (QUIAGEN®) was based on alkaline lyses of bacterial cells followed by adsorption of DNA onto silica in the presence of high salt.

This protocol is designed for purification of up 20 µg of high-copy plasmid DNA from 1-5mL overnight culture of *E. coli* in LB medium.

The volume of 1,5mL of culture was added into a microcentrifuge tube and centrifuged at maximum speed for 1 minute. After centrifugation, the medium was removed by aspiration leaving the bacterial pellet at the bottom. This procedure was repeated twice. The bacteria pellet was then resuspended in 250µL of Buffer P1, which contains RNAase. Once no cells clumps were visible in suspension, 250µL of Buffer P2 was added and the tube was gently inverted 4-6 times to mix, but not allowing the lyses reaction to proceed for more than 5 min. In order to stop the lyses reaction, 350µL of Buffer N3 was added and the tube was inverted 4-6 times immediately but gently until the solution becomes cloudy. The tube was centrifuged for 10 min at maximum speed, and a compact white pellet was observed. The supernatant was removed by pipetting and placing into the QIAprep column®, following centrifugation for 30-60s and the discard of the flow-through. In order to wash the spin column, 750µL of Buffer PE was added and centrifugation was performed for 30-60 s. The flow-through was discarded and the column was centrifuged for an additional 1 min to remove residual wash buffer. In order to elute the DNA, the column was placed in a clean 1,5mL microcentrifuge tube and 50µL of Buffer EB (elution buffer) was added to the center of each QIAprep column®, let stand for 1-3 min, and centrifuged for another 1min.

2.4.1.4 Plasmid Linearization

Most of the common vectors contain promoters for T3 and T7 RNA polymerases at each end of the polylinker. 3 to 10µg of the vector were linearized for 3 hours at 37ºC with the appropriated restrictions enzymes and buffers commercially supplied (Roche®). After digestion, the efficiency of the restriction was checked in a 1% agarose gel using 1/20 of the digestion reaction volume.

2.4.1.5 Anti-sense RNA probe Transcription

Plasmids containing cDNA of the chosen molecular markers and single stranded RNA probes were generated by *in vitro* transcription from a linearized DNA template using the appropriated restriction enzymes that cut at the 5'end, SP6, T3 and T7 (Roche®).

DNA inserts corresponding to the gene of interest (total or partial) were transcribed using an according RNA polymerase (T3, T7 or SP6) (Roche®) in order to produce an antisense transcript, which synthesizes RNA complementary to the DNA template.

In a RNAase free tube, 1-2µg of DNA linearized plasmid (approximately 200ng), 2µL of transcription buffer (Roche®), 2µL of 10X Digogenin labeling mix (DIG), 1µL of RNAout (Promega®) to avoid RNA degradation and 1µL of RNA Polimerase were added under RNAase free conditions. RNAase free water was added to make up a final volume of 20µL.

The transcription reactions were incubated at 37ºC during 3 hours.

The list of the probes used, and how they were made is in appendix.

2.4.1.6 Anti-sense RNA probe clean up

The mini Quick Spin columns (Roche®) are gel filtration columns, which separate molecules based on their relative size by chromatographic separation. The matrix was initially resuspended in the column buffer by gentle vortex. The excess buffer was removed and the column beads were packed by centrifugation for 1min in a microcentrifuge at 1000x g. The Anti-sense RNA probe was then applied to the center of the column beads, followed by the centrifugation of the column for 4 min at 1000x g at 4ºC. The sample was collected in a microcentrifuge tube and stored at -20ºC. 1µL of the probes was run on a 2% agarose gel in order to confirm if the transcription reaction was successful.

2.4.2 Embryos or kidneys pre-treatments

Embryos and kidneys were rehydrated through a series of 75, 50 and 25% methanol in PBSwDEPC and finally were rinsed twice in 100% PBSwDEPC. The embryos and kidneys were bleached in 6% hydrogen peroxide (freshly made in PBSwDEPC), for 1 hour in the dark, at RT. After this embryos and kidneys were washed three times for 5 min with PBSwDEPC. Subsequently, the biological material was digested with Proteinase K (PK) and incubated with 10 µl/mL pK, in PBSwDEPC (the period of incubation depended on the embryonic stage, see appendix). In order to inhibit the proteinase K, a washing in freshly prepared 2mg/mL glycine in PBSwDEPC was performed during 5 min. After rinsing, the embryos and kidneys were refixed (post-fix) in 4% PFA (paraformaldehyde) and 0.2% glutaraldehyde in PBSwDEPC for 15 min. Next, the embryos and kidneys were again rinsed in PBSwDEPC for 5 min, on three times.

2.4.3 Hybridization

Hybridization comprises several steps. First the embryos must be incubate with a pre-hybridization solution (see appendix) at 72ºC during at least 3 hours, period in which the solution can penetrate into the cells and the optimal temperature to the hybridization is achieved. After this period, the hybridization solution is prepared using the same mixture as the pre-hybridization solution and adding the appropriate antisense probe, tRNA and ssDNA (see appendix), followed by a RNA secondary structures denaturation step for 10min at 72ºC. The embryos are then incubated with the hybridization solution in a moisturized environment. The hybridization itself was carried out O/N, at 72°C.

2.4.4 Antibody Incubation

Initially, hybridization solution was removed, and the embryos and kidneys were rinsed 2 times each with pre-heated solution I and II (see appendix) during 30 a 45 min at 65ºC. WISH solution I was removed and replaced by WISH solution II. Subsequently, they were rinsed 3 times with maleic acid buffer, 0,1% Tween-20%

(MABT, see appendix) solution for 5 minutes at RT on the rocker. In order to block unspecific antibody binding sites, the embryos were incubated with WISH blocking solution (see appendix) for 2 hours at RT in a rocker. Blocking solution was removed and then incubated with WISH antibody (Roche®) solution (see appendix) at 4ºC ON rocking with smooth agitation.

2.4.5 Immunological Detection

The antibody solution was removed and the embryos and kidneys were washed 5 times with MABT and the solution was changed every 45 min. The embryos and kidneys were then washed twice for 10 min with the buffer, NTMT (see appendix), in the roller at RT. Finally, NTMT solution was removed and the embryos and kidneys were incubated in the developing solution (BMpurple or BCIP, Roche®). The detection reaction was carried out in the dark at room temperature. After verifying if the embryos and kidneys have a good immunological signal in stereoscope, the reaction was stopped by removing the developing solution and adding PBS solution changed twice.

In the case of a WISH where a single probe is used, the embryos and kidneys were photographed, post-fixed, dehydrated and subsequently stored at -20ºC.

2.5 Histology

The embryos were used for histology after mRNA *in situ* hybridization so we proceeded with a paraffin inclusion for following microtome sectioning. In the case of the kidneys histology, after paraffin inclusion, they were stained hematoxilin-eosin.

2.5.1 Paraffin embedding

After dissection or mRNA in situ hybridization the embryos or kidneys were fixed in 4% PFA ON. On the next day, the embryos or kidneys were dehydrated through a series of methanol:PBSwDEPC 25%, 50%, 75% and 100%. Subsequently, the samples were kept in isopropanol during 15 min at 68^{o}C. Afterwards, the biological material

was kept in isopropanol:paraffin (1:1) during 30 min at 68ºC and then in liquid paraffin during 1 hour. Finally, the embryos or kidneys were placed in mold ON in liquid paraffin at 68ºC.

On the next day, the embryos or kidneys were orientated in mold according to the desired orientation. The paraffin was solidified at RT and the molds were stored at 4ºC. Depending on the size of the embryos, sections were performed from a range of 6µm to 10µm.

2.5.2 Kidney Histology - Processes of Hematoxilin-Eosin

Kidneys were removed and fixed ON in 4% PFA, after what they were included according to what is described in section 2.5.1. Sections were performed at 6 µm. After the sectioning, paraffin was removed by washing twice with xylene for 10 and 5 min each at RT. Sections were then rehydrated through an ethanol series of washes from 100% during 2 and 1min, subsequently 96% during 2 min, and 70%, 2 min for each step, and then washed in distilled water for 3 min. The tissues were stained using the hematoxilin and eosin. Sections were immersed for 5 min in hematoxilin, and washed with water for 3 min. Then the samples were briefly wash with 70% ethanol and 0,5% hydrochloride acid. Following, they were immersed in water for 1 min and then with 70% ethanol. Subsequently, the sections were immerged in eosin during 2 min. Sections were then dehydrated through graded ethanol series (twice at 100% ethanol and 96%, 2 minutes each), and then immerse in xylene twice for 5 min each. Slides were mounted with DPX (Fluka®). After 24h sections were analyzed at the Axio Observer Z2 Fluorescence microscope®.

2.6 Skeletal Analysis

To perform the skeletal analysis of the newborns, Alcian blue/Alizarin red staining was applied according to what is described in Belo et al. (1998). Skin and viscera were removed from the neonates mice, and the tissue was fixed ON in ethanol 95%. On the following day the remaining tissues were stained for three days with 0,045% Alcian blue (), 80% ethanol and 20% acetic acid. After three days, alcian stain

was washed with 95% ethanol for 6h. This solution was then replaced with 2% KOH for 24h. Specimens were stained with 0,03% Alizarin red (Sigma) in 1% KOH for 12h and were cleared with 1% KOH, 20% glycerol, and passed through a glycerol/ethanol storage solution series: 50%, 80% and finally 100% glycerol.

2.7 Photography

All embryos and kidneys after dissection or *in situ* hybridization were photographed with a SteREO Lumar.V12 Fluorescence Stereomicroscope®. The histological sections were photographed with an Axio Imager Z2 Fluorescence microscope®. Images were processed or treated using Adobe Photoshop® software.

3 Results

In order to better understand the *Adtk1* phenotype during mouse development we are currently carrying out several types of experiments. Following, it will be present the different types of crosses and their genotyping and the obtained results for each one.

3.1 Phenotype analyses in C57Black6 strain

After the reported results on Gonçalves, et al (2011)[86], Imuta, et al (2009)[92] and Kinoshita, et al (2009)[93], our laboratory has continued the study of the *Adtk1* gene in mouse development.

3.1.1 Study Newborns *Adtk1*$^{-/-}$ in C57Black6 mouse

Aiming to achieve double-mutant newborns for the *Adtk1* gene continuing the study published by Lisa Gonçalves et al (2011), females were crossed with males, all heterozygous for the gene *Adtk1*. However, starting from the first 37 births referred in Gonçalves et al (2011), we did not obtain the birth of knock-out (KO) newborns as shown in the following table. 202 newborns were gathered from crosses *Adtk1*$^{+/-}$ C57BL6, immediately after birth, which were genotyped, but no *Adtk1*$^{-/-}$ newborns were obtained (table 2).

Tabela 2 – Number of newborns obtained by the cross of *Adtk1*$^{+/-}$ in C57BL6.

Type of cross	Stage which they were collected	Total Number	Wild-type	Heterozygos	Homozygous	Ungenotyped
Adtk1$^{+/-}$ C57Bl6	Newborns	202 (100%)	46 (22,8%)	156 (77,2%)	0 (0%)	0 (0%)

Since on the first experiment, from the cross of two heterozygous for the *Adtk1* gene in C57Bl6 strain did not resulted in any *Adtk1*$^{-/-}$ in the newborn stage, we

suspected that an intrauterine death could be occurring. Because of this hypothesis, we began dissecting the females during the embryonic development, and started looking for intrauterine death, through the presence of empty decidua (placenta where the dead embryo is reabsorbed by the mother) in all litters dissected. Therefore we started by dissecting the E13.5, E12.5 and E10.5 in the hope of finding *Adtk1*$^{-/-}$ embryos at these stages, but we still continued with an absence of KO embryos. Yet we continued to see empty decidua in almost all dissected females. This indicated that it was more likely that the embryos were dying earlier than the analyzed stages to date (Table 3).

Tabela 3 - Number of embryos obtained by the cross of *Adtk1*$^{+/-}$ in C57BL6 dissected at stages E11.5-E13.5.

Type of cross	Stage which they were collected	Total Number	Wild-type	Heterozygos	Homozygous	Ungenotyped
Adtk1$^{+/-}$ C57Bl6	E13.5	38 (100%)	8 (21%)	30 (79%)	0 (0%)	0 (0%)
Adtk1$^{+/-}$ C57Bl6	E12.5	42 (100%)	11 (26%)	31 (74%)	0 (0%)	0 (0%)
Adtk1$^{+/-}$ C57Bl6	E11.5	36 (100%)	9 (25%)	27 (75%)	0 (0%)	0 (0%)

As can be seen in Table 3 in the E13.5 several litters were dissected and a total of 38 embryos were obtained. 8 (21%) of them were wild-type for *Adtk1* gene and 30 (79%) were *Adtk1*$^{+/-}$ gene. There wasn't any KO embryo for *Adtk1* gene.

At E12.5 several litters were dissected and a total of 42 embryos were obtained. 11 (26%) of them were wild-type *Adtk1* gene and 31 (74%) were

heterozygous for this gene. In this stage we also didn't obtained any knock-out embryo.

Due to the lack of *Adtk1*$^{-/-}$ embryos, we started dissecting several embryos at E11.5 and we obtained a total of 36 embryos. 9 (25%) of them were wild-type for *Adtk1* gene, 27 (75%) were heterozygous for the *Adtk1* gene and we also didn't obtained any *Adtk1*$^{-/-}$ embryos

Since no *Adtk1*$^{-/-}$ embryos were obtained on the previously analyzed stages, we started then dissecting at E9.5 and E10.5. As can be seen in table 4, we did not obtain *Adtk1*$^{-/-}$ embryos in E10.5 but in E9.5 we found 2 *Adtk1*$^{-/-}$ embryos.

Tabela 4 - Number of embryos obtained by the cross of *Adtk1*$^{+/-}$ in C57BL6 dissected at stages E9.5-E10.5.

Type of cross	Stage which they were collected	Total Number	Wild-type	Heterozygos	Homozygous	Ungenotyped
Adtk1$^{+/-}$ C57Bl6	E10.5	48 (100%)	16 (33%)	32 (67%)	0 (0%)	0 (0%)
Adtk1$^{+/-}$ C57Bl6	E9.5	59 (100%)	9 (15%)	48 (81%)	2 (4%)	0 (0%)

In the E10.5 we obtained a total of 48 embryos.16 (33%) of them were wilt-type for *Adtk1* gene and 32 (67%) were heterozygous for this gene. None knock-out embryo was obtained.

When we started the dissection at E9.5, in 59 embryos, 9 (15%) of them were wild-type for the *Adtk1* gene and 48 (81%) were heterozygous for the *Adtk1* gene. At this stage, we obtained two KO embryos (4%). Following, the analysis of these embryos will be described.

3.1.2 Analyze of Embryos in E9.5 *Adtk1*$^{-/-}$ C57Black6

When we began to dissect the embryos at E9.5, in 59 of them 2 where *Adtk1*$^{-/-}$ and seemed to have an open neural tube in the middle (Figure 16). Images were then collected after dissection without any treatment (Figure 16).

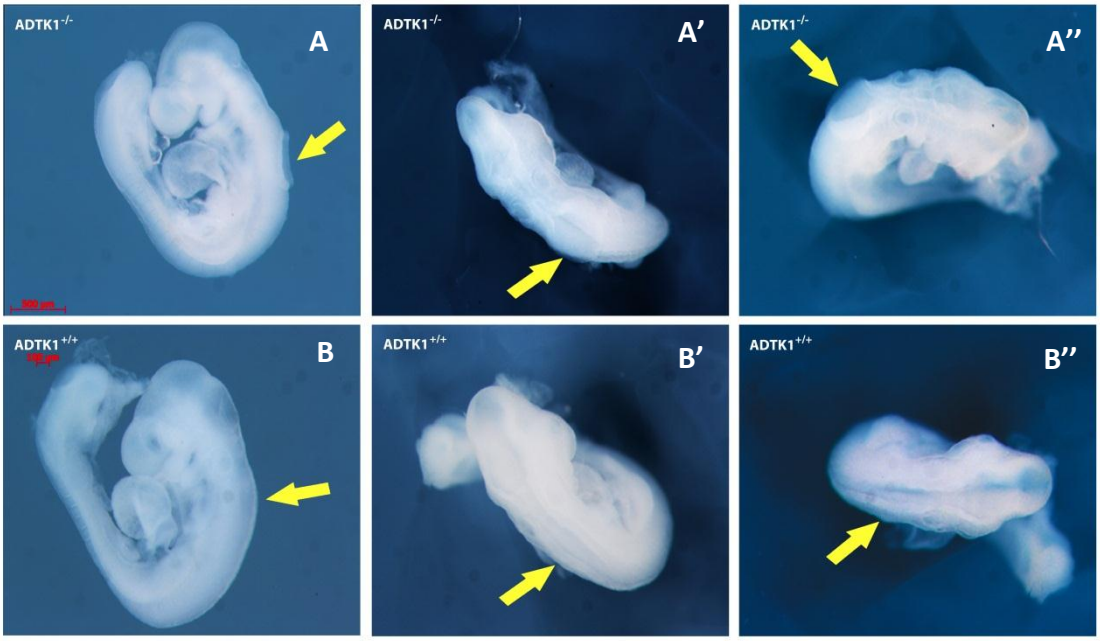

Figure 16: *Adtk1* KO induces neural tube defects. (A-B'') Embryos at E9.5. Comparing the *Adtk1* KO embryos (A-A'') with wild-type embryos (B-B'') it is possible to observe defects in neural tube in the absence of the *Adtk1*. A and B are left lateral views and A',A'',B' and B'' are dorsal views.

Comparing the *Adtk1*$^{-/-}$ embryo (A-A'') with wild type embryo (B-B'') it is possible to observe that the neural tube is not properly closed (yellow arrow, A-A''). The neural tube starts to close from posterior to anterior,[1] but in *Adtk1*$^{-/-}$ embryos, the neural tube is closed in the posterior and anterior regions but fails to close in the middle between this two regions.

Due to the suspicion that the E9.5 KO embryos had defects in the neural tube we began researching genes that would mark the closing of the neural tube at E8.5 and

E9.5 in order to better identify the obtained phenotype. We began by performed an *in situ* hybridization with a known marker. Since apparently the observed defect was in the neural tube closure we selected the *Noggin* gene, which marks at E9.5 the 1st arch mesenchyme mandibular part, spinal cord neural tube, 1st arch ectoderm mandibular part [36].

In order to obtain the *Noggin* probe, a small amount of DNA plasmid that we had in stock in the laboratory was transformed in *E. coli* (TOP10®). To get the *Noggin* in a plasmid, the steps described in (2.4.1 Materials and methods) were performed. After the construction of an antisense RNA probe, the experimental procedure for *in situ* hybridization (2.4.2 to 2.4.5) was carried out. The obtained results were subsequently photographed with a Fluorescence Stereomicroscope SteREO Lumar.V12 ®, figure 17.

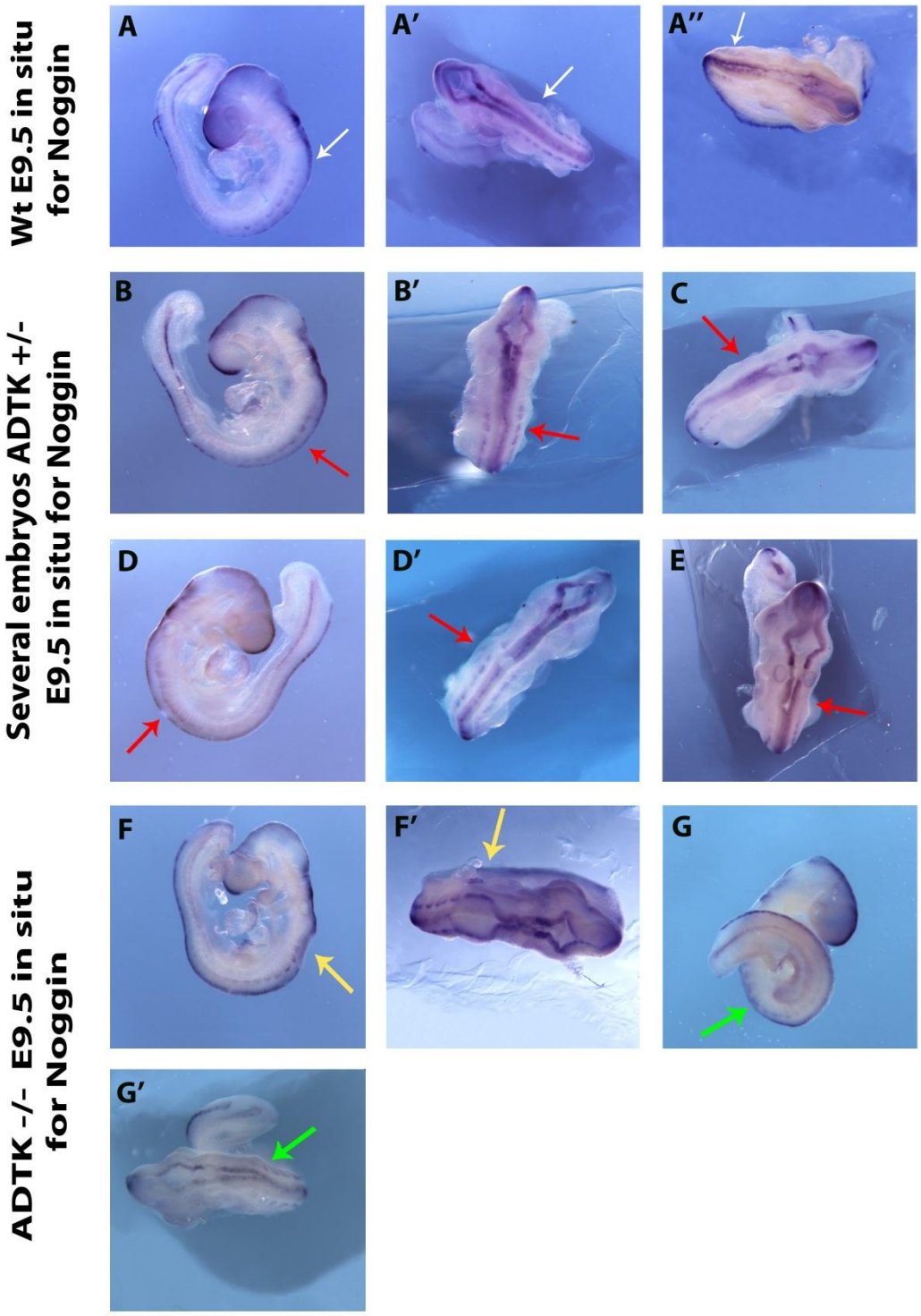

Figure 17: In situ hybridization at E9.5 for *Noggin.* In the absence of *Adtk1* gene, the embryo develops with neural tube closure defects (yellow and green arrows; F-G') comparing with wild type embryos (A-A''). In *Adtk1*$^{+/-}$ embryos it is possible to observe a slightly delay in neural tube closure (red arrow; B-E) compared with wild type embryos (A-B''). A, B, D, F, and G are lateral views and A',A'',B', C, D', E, F' and G' are dorsal views.

Comparing the *Adtk1* $^{-/-}$ embryos with wild type embryos (A-A'') hybridized with *noggin*, it is possible to better observe the region of neural tube that is not properly closed (yellow arrow F-G'). In one of the two *Adtk1*$^{-/-}$ obtained the embryo also seems to be smaller than the wild type embryos. However the neural tube is not opened like the other *Adtk1*$^{-/-}$ embryo but its closure is delayed (green arrow) compared with the wt embryos. In the case of embryos *Adtk1*$^{+/-}$, a delay on neural tube closure could be observed (red arrow) compared with wild type embryos.

In order to better clarify the obtained phenotype the embryos *in situ* hybridized with the Noggin were sectioned in a microtome at 10µm (histology, materials and methods). The sections are visible in figure 18 below.

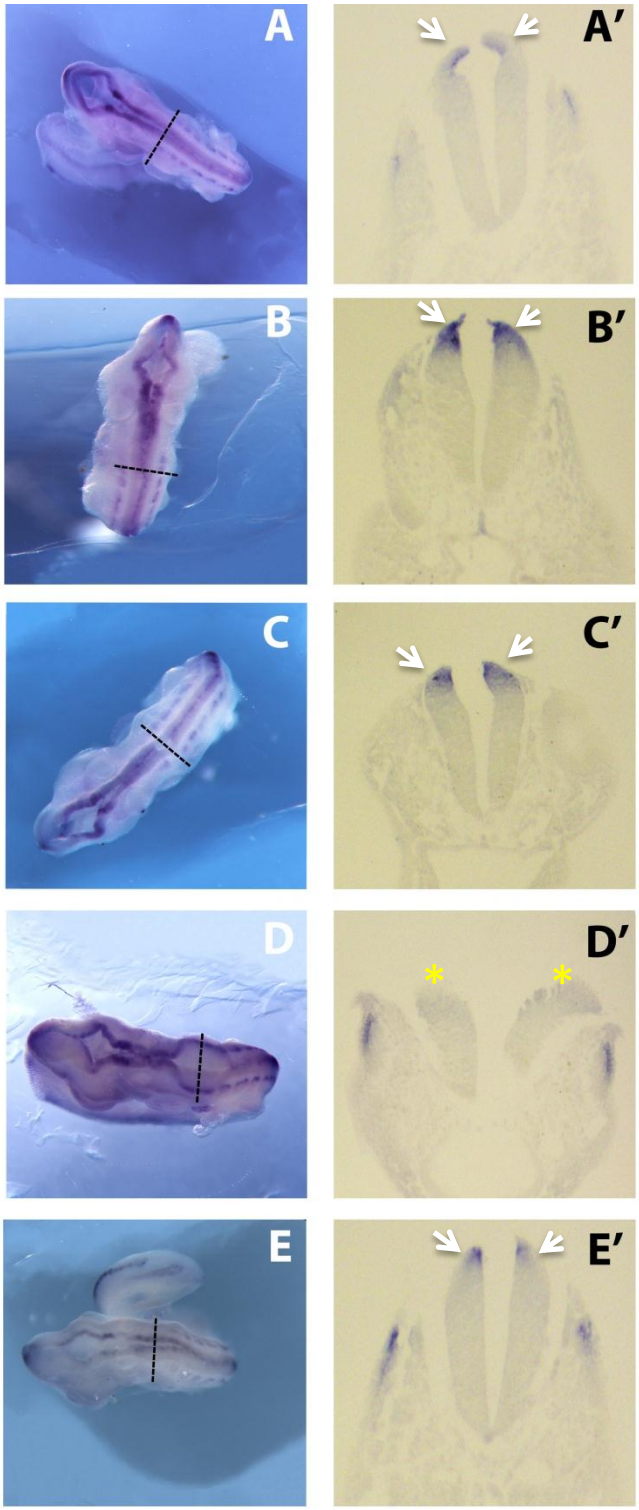

Figure 18: *Adtk1* absence disrupts neural tube closure at E9.5. Whole-mount in situ hybridization with Noggin (A-E) and sections of these embryos (A'-E'). In the *Adtk1*$^{-/-}$ embryos it is possible to observe neural tube closure defect. While in one KO embryo (E) the neural tube is not correctly closed but the phenotype is mild in the other *Adtk1*$^{-/-}$ embryo the neural tube has an open area between anterior and posterior region (D). *Adtk1*$^{+/-}$ presents a delay in neural tube closure (B-C').

In the *Adtk1*$^{-/-}$ embryos, at E9.5 it is possible to observe neural tube closure defect. While in one KO embryo (E) the neural tube is not correctly closed but the phenotype is mild (E') in the other *Adtk1*$^{-/-}$ embryo the neural tube has an open area between anterior and posterior region (D). This could be better observed in sections (D') where the neural tube is completely open in this region and Noggin it is not expressed in the roof plate (yellow *) like in wild-type embryo (A and A'). In *Adtk1*$^{+/-}$ embryos (B and C) the neural closure seems to be delayed (B' and C') compared with wild-type embryo (A'). However, *Adtk1*$^{+/-}$ embryos recover from this delay in neural tube closure since they born without any defect related with neural tube closure defects.

3.1.3 Analyze of Embryos in E6.5 to E8.5 *Adtk1*$^{-/-}$ C57Black6

Following the observed embryonic lethality in the newborns genotyped we started dissecting along the embryonic development in E6.5 to E8.5.

Tabela 5 - Number of embryos obtained by the cross of *Adtk1*$^{+/-}$ in C57BL6 dissected at stages E6.5-E8.5.

Type of cross	Stage which they were collected	Total Number	Wild-type	Heterozygos	Homozygous	Ungenotyped
Adtk1$^{+/-}$ C57Bl6	E8.5	11 (100%)	3 (27%)	6 (55%)	1 (9%)	1 (9%)
Adtk1$^{+/-}$ C57Bl6	E7.5	8 (100%)	1 (12,5%)	6 (75%)	0 (0%)	1 (12,5%)
Adtk1$^{+/-}$ C57Bl6	E6.5	9 (100%)	3 (33,3%)	3 (33,3)	2 (22,2%)	1 (11,1%)

In the E8.5 stage, a total of 11 embryos were obtained. 3 (27%) of them were wild-type for the *Adtk1* gene and 6 (55%) were heterozygous for the *Adtk1* gene, there

was 1 *Adtk1*$^{-/-}$ embryos at this stage (9%) and in one of the embryos the genotyping was not conclusive so this embryo was considered ungenotyped.

When we started the dissection at E7.5 in 8 embryos, 1 (12,5%) of them was wild-type for the *Adtk1* gene and 6 (75%) were heterozygous for the *Adtk1* gene. At this stage we did not obtained any KO embryos and in one of the embryos the genotyping was not conclusive so this embryo was considered ungenotyped.

At the E6.5 we obtained a total of 9 embryos. 3 (33,3%) of them were wild-type for the *Adtk1* gene and 3 (33,3%) were heterozygous for the *Adtk1* gene, there were 2 KO embryos at this stage (22,2%) and in one of the embryos the genotyping was not conclusive so this embryo was considered ungenotyped.

Following, the analysis of the E8.5 and E6.5 embryos in *Adtk1*$^{-/-}$ C57BL6 strain will be described.

3.1.4 Analyze of Embryos in E8.5 *Adtk1*$^{-/-}$ C57Black6

When we started to dissect at E8.5 we found that in 11 embryos just only one was KO with many phenotypic deformities.

To further clarify the obtained phenotype we started an *in situ* hybridization with the known marker *Fgf8*. This marker was selected, because the *Fgf8* gene is expressed at stage 8.5 in the foregut diverticulum, future prosencephalon, optic sulcus neural ectoderm[94].

In order to obtain the *Fgf8* probe, a small amount of DNA plasmid that we had in stock in the laboratory was transformed in *E. coli* (TOP10®). To get the *Fgf8* in a plasmid the steps described in (2.4.1 Materials and Methods) were performed. After the construction of an antisense RNA probe the experimental procedure in situ hybridization (2.4.2 to 2.4.5) was carried out. The obtained results were subsequently photographed with a Fluorescence Stereomicroscope SteREO Lumar.V12 ®, figure 18.

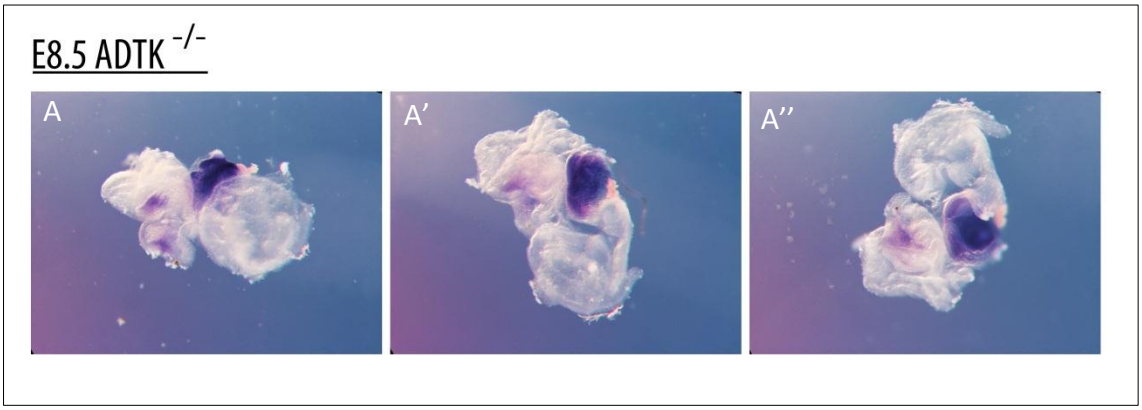

Figure 19*: In situ* hybridization for *Fgf8* at E8.5 (A-A''). The *Adtk1*$^{-/-}$ embryo found at stage E8.5 is very abnormal.

During the dissections it was very important to find a KO at E8.5, however few embryos were dissected at this stage. The only KO embryo that was found did not reveal to be clarifying since it was very deformed not allowing us to see the different structures that constituted the embryo. However, the mFGF8 marker was restricted to a very specific place what seemed to be very interesting. Nevertheless, this is a preliminary result that needs to be further analyzed through the dissection of more embryos at this stage.

3.1.5 Analyze of Embryos in E6.5 *Adtk1*$^{-/-}$ C57Black6

When we begin to dissect at E6.5 embryos we found in 9 of them 2 *Adtk1*$^{-/-}$ with apparently little phenotypic changes.

To further understand the obtained phenotype we performed an *in situ* hybridization with the known marker, *Fgf8*. This marker was also selected because the *Fgf8* gene is expressed at E6.5 in the primitive embryonic endoderm and primitive streak [95].

In order to obtain the *Fgf8* a small amount of DNA plasmid that we had in stock in the laboratory was transformed in *E. coli* (TOP10®). To get the *Fgf8* in a plasmid the steps described in (2.4.1 Materials and Methods) were performed. After the construction of an antisense RNA probe the experimental procedure in situ hybridization (2.4.2 to 2.4.5) was carried out. The obtained results were subsequently photographed with a Fluorescence Stereomicroscope SteREO Lumar.V12 ®, figure 20.

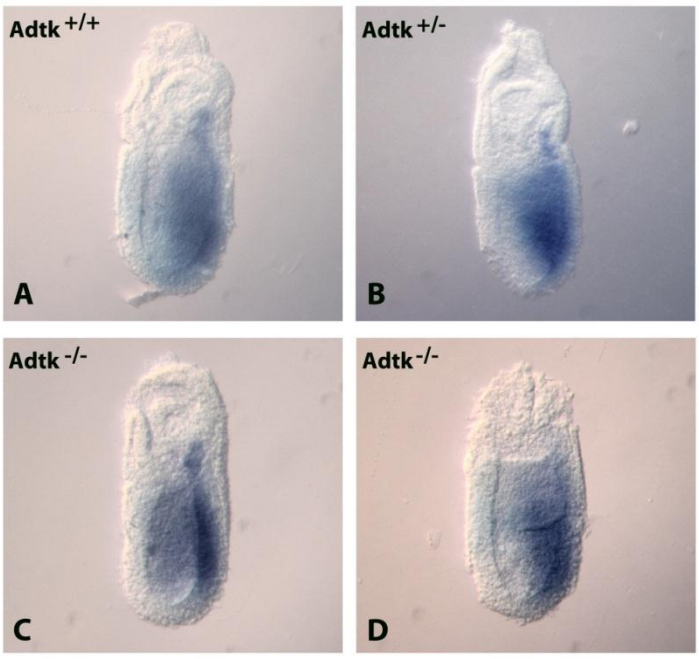

Figure 20: In situ hybridization for *Fgf8* at E6.5. A is a wild-type embryo, B is a heterozygous embryo and C and D are a KO embryo for the Adtk1 gene. Both *Adtk1*$^{-/-}$ and *Adtk1*$^{+/-}$ apparently are similar to wild type embryos.

After *in situ* hybridization with *Fgf8* gene analyses we observed that the *Adtk1*$^{-/-}$ embryos are apparently similar to wild type embryos. However it is necessary to dissect more embryos in this stage to clarify the lack of phenotype since later the embryos present some developmental defects.

3.2 Phenotype Analyses in Hybrid Background

On the first experiment, two *Adtk1* heterozygous C57Bl6 were crossed and we didn't obtain any knockout newborns. However, after some paper research, we

observed that some authors were able to obtain Adtk1-/- newborns(*Pkdcc*[92] and *Vlk*[93]). Following this, we decided to investigate which strains they used to generate these Adtk1-/- mice newborns. Could it be because they used an hybrid background?

When we reviewed the *Vlk* gene paper [93]we observed that it was not present the information of each type of cells was injected to generate the mutant mouse. However, when analyzing the paper with the *Pkdcc* gene,[92] we found that the animals had a hybrid background. They used TT2 ES cells to inject the blastocysts (cells from the embryos resulting from the cross between a C57BL6 female and a CBA male.[96] Therefore the *Pkdcc* newborns analyzed in the paper had a hybrid background with the CBA and C57BL6 strains.

After this analysis in an attempt to try to obtain KO newborns for the *Adtk1,* gene we decided to generate a hybrid background. With the aim of obtaining hybrid knockout newborns we crossed *Adtk1*$^{+/-}$ C57BL6 mice with a 1stDBA. DBA mice were the directory to use instead of CBA mice only by a matter of availability, since the animal facility of the University of the Algarve only disposed these animals. From this cross we obtained the F1 generation, *Adtk1*$^{+/-}$C57BL6;1stDBA. In adulthood, the heterozygous mice were crossed with each other resulting in the F2 generation. This generation was collected soon after birth and analyzed in search of *Adtk1*$^{-/-}$ mice (genotyping), table 6.

Tabela 6 - Number of newborns obtained by the cross of *Adtk1*$^{+/-}$ in C57BL6/1stDBA

Type of cross	Stage which they were collected	Total Number	Wild-type	Heterozygos	Homozygous	Ungenotyped
Adtk1$^{+/-}$ C57Bl6; 1stDBA	Newborns	110 (100%)	38 (35%)	70 (64%)	2 (1%)	0 (0%)

In 110 analyzed newborns 38 (35%) of them were wild-type for *Adtk1* gene and 70 (64%) were heterozygous for this gene. There were 2 *Adtk1*$^{-/-}$ newborns (1%).

Because the percentage of obtained newborns KO was very low (1%),it was decided to generate a second hybrid background. With the aim of obtaining hybrid *Adtk1*$^{-/-}$ newborns we crossed *Adtk1*$^{+/-}$C57BL6;1stDBA, with DBA mice. From this cross the obtained F1 generation that was *Adtk1*$^{+/-}$C57BL6;2ndDBA. In adulthood, the heterozygous mice were crossed with each other resulting in a F2 generation. This generation was collected soon after birth and analyzed in search of *Adtk1*$^{-/-}$ mice (genotyping), table 7.

Tabela 7 - Number of newborns obtained by the cross of *Adtk1*$^{+/-}$ in C57BL6/2ndDBA.

Type of cross	Stage which they were collected	Total Number	Wild-type	Heterozygos	Homozygous	Ungenotyped
Adtk1$^{+/-}$ C57Bl6; 2ndDBA	Newborns	102 (100%)	36 (35%)	66 (65%)	0 (0%)	0 (0%)

In 102 analyzed newborns, 36 (35%) of them were wild-type for the *Adtk1* gene and 66 (65%) were heterozygous for this gene. In this hybrid background, until now we did not obtain any *Adtk1*$^{-/-}$ embryos.

Because we didn't obtain any *Adtk1*$^{-/-}$ newborn, we decided to perform another cross with *Adtk1*$^{+/-}$ 129sv mice. However, we are still waiting for the births in this background.

3.2.1 Gene *Adtk1* expression in Kidneys

Previously we observed that the *Adtk1* gene was expressed through the renal embryonic development.

To better understand its expression we performed an *in situ* hybridization for the *Adtk1* gene. In order to obtain the *Adtk1* a small amount of DNA plasmid that we had in stock in the laboratory was transformed in *E. coli* (TOP10®). To get the *Adtk1* in a plasmid the steps described in (2.4.1 Materials and methods) were performed. After the construction of an antisense RNA probe the experimental procedure in situ hybridization (2.4.2 to 2.4.5) was carried out. The obtained results were subsequently photographed with a Fluorescence Stereomicroscope SteREO Lumar.V12 ®, figure 21.

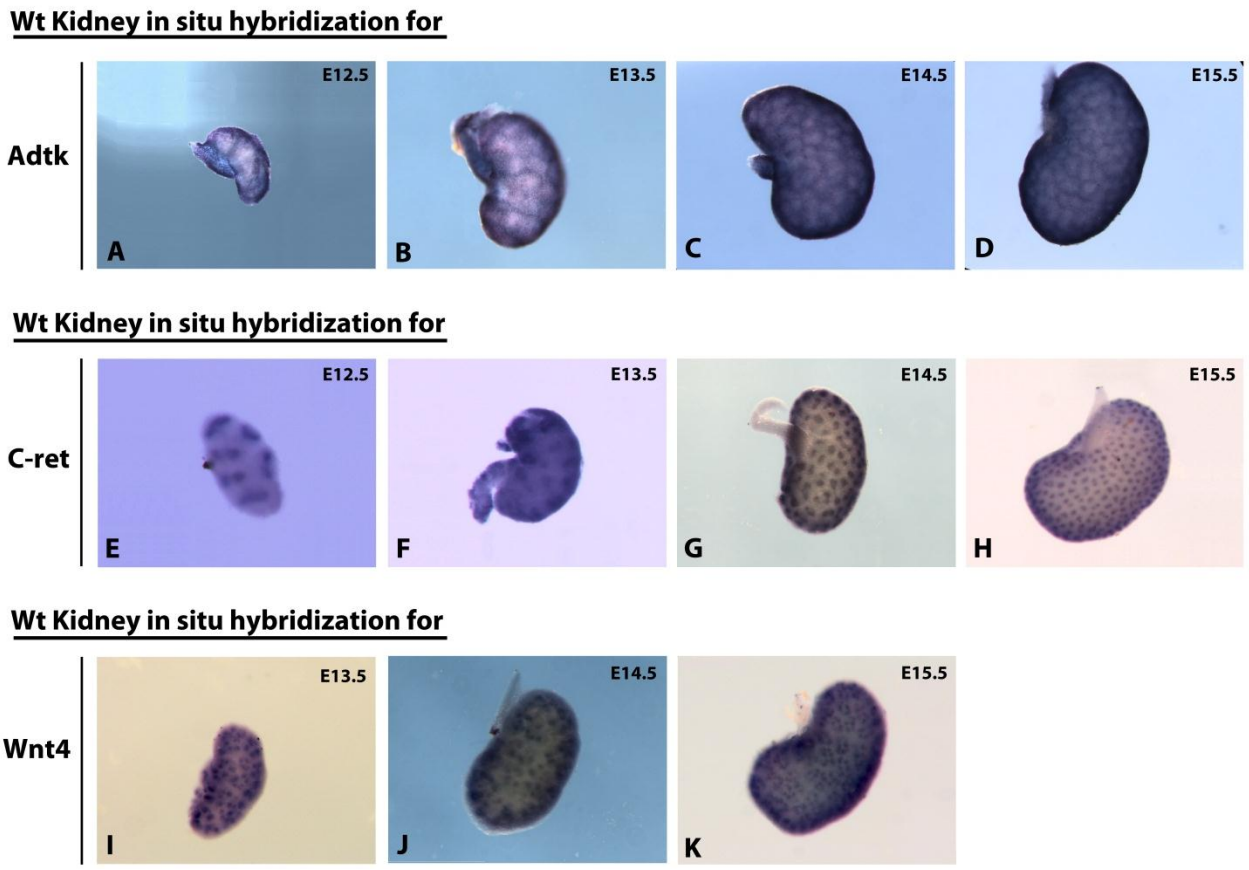

Figure 21 – *In situ* hybridization for different kidneys markers from E12 to E15.5 in wild-type mice. *Adtk1* from A to D, *C-ret* from E to H and *Wnt4* from I to K.

In a preliminary study we described the expression pattern of *Adtk1* gene in kidney development. With this purpose we performed in situ hybridization for the *Adtk1* between stages E12.5 and E15.5. We observed that *Adtk1* is expressed like a net in the glomerulus region.

3.2.2 Other Genes Involved in Kidney Development

More than 400 genes are known to be expressed during nephrogenesis. Several signaling pathways are involved in kidney development. In our context the kidney and its signaling pathways are very interesting because the development of kidneys in the *Adtk1* knock-out mice (*Adtk1*$^{-/-}$) seem to be affected by the absence of this gene. In this work particular attention was given to the relationship between *Wnt4*, *C-RET* and and *Adtk1* genes since they are related to kidney development.

To further clarify the above mentioned genes expression we performed an *in situ* hybridization. In order to obtain the *Wnt4*, *C-RET* and *Adtk1* genes a small amount of DNA plasmid that we had in stock in the laboratory was transformed in *E. coli* (TOP10®). To get the *Wnt4*, *C-RET* and *Adtk1* genes in a plasmid the steps described in (2.4.1 Materials and methods) were performed. After the generation of an antisense RNA probe the experimental procedure *in situ* hybridization (2.4.2 to 2.4.5) was carried out. The obtained results were subsequently photographed with a Fluorescence Stereomicroscope SteREO Lumar.V12 ®, Figure 21

By in situ hybridization we observed that C-ret is a gene expressed in the kidneys in the uretic bud (UB)[97] and *Wnt4* is expressed in pronephros[98]. However, *Adtk1* is not expressed in the same structures that these genes, being expressed in the glomerulus region.

3.2.3 Analysis of *Adtk1*$^{-/-}$ Mutants in the Hybrid Background C57Bl6/1stDBA

In 110 analyzed newborns in the hybrid background C57Bl6;1stDBA, 38 (35%) of them were wild-type for the *Adtk1* gene and 70 (64%) were heterozygous for this gene. There were 2 *Adtk1*$^{-/-}$ newborns (1%) (figure 22).

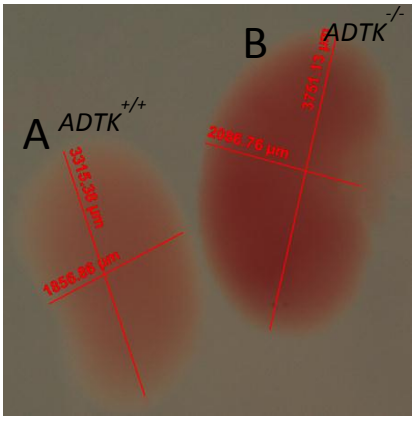

Figure 22: *Adtk1* null mutants present defects in kidney morphology. (A) Wild-type, (B) *Adtk1*$^{-/-}$. Knock-out kidney is bigger than wild-type and more reddish.

The *Adtk1*$^{-/-}$ newborns kidneys show differences compared with wild-type newborn kidneys. The KO kidneys are bigger than wild-type and more reddish. Because of that, we want to verify which tissues are affected by the absence of *Adtk1*. With this purpose, we sectioned the embryos at 10 µm and we analyzed their kidneys histology (figure 23).

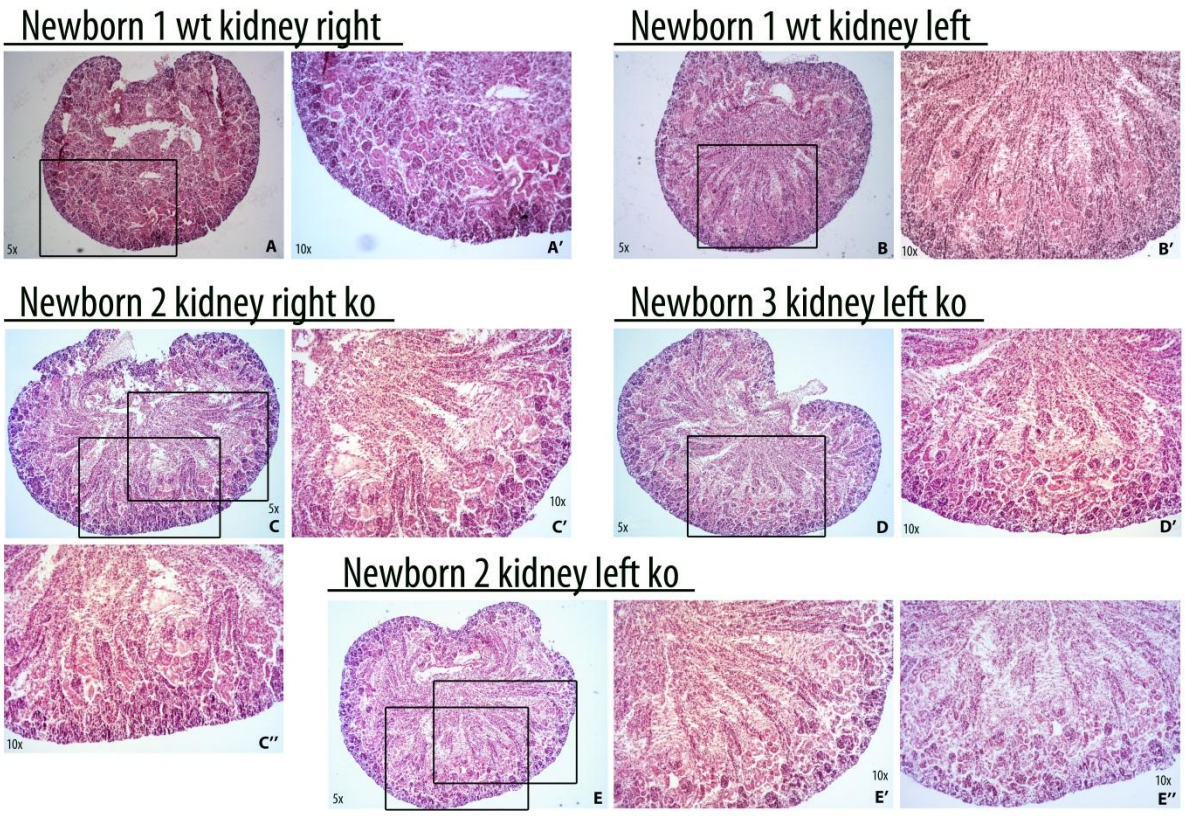

Figure 23: Kidney histology with hematoxilin-eosin. Wild-type newborns kidneys (A-B') and *Adtk1*$^{-/-}$ newborns kidneys (C-E''). Amplification of 10X (A,B,C and D) and 5X (A', B', C', C'', D', E' and E''). The *Adtk1* $^{-/-}$ newborn kidneys demonstrated defects in the glomerulus and medullar zone namely gaps when compared with wild type kidneys.

When we compare the section of kidney *Adtk1*$^{-/-}$ with wild-type, it is possible to observe that *Adtk1*$^{-/-}$ kidneys present several defects. These kidneys showed gaps between the glomerulus and medullar zone, and cortex region presents empty spaces that is not visible in wild type kidneys. In these kidneys the medullar zone seems to be more compact than in *Adtk1*$^{-/-}$ kidneys.

Data presented by Imuta, et. al. (2009), showed that *Adtk1* (Pkdcc) knockout mice exhibited shorter limbs than its wild-type littermates. The skeleton of Adtk1 mutant specimens were analyzed and we observe that the bones presented differences in length,[77] although mild ones comparing to Imuta (2009). This author

reported bone defects in Pkdcc mutants,[83] however, until now all null mutants obtained in our lab were roughly the same size as its wild-type littermates and no obvious differences were noticed. However, skeletal analysis with alizarin red and alcian blue provided further and more detailed information. In Adtk1-/- limbs, the mineralized regions, which stained red with alizarin red, were significantly shortened compared with its wild type littermates, whereas the size and morphology of the cartilage, which stained blue with alcian blue, were not significantly affected (Figure24).

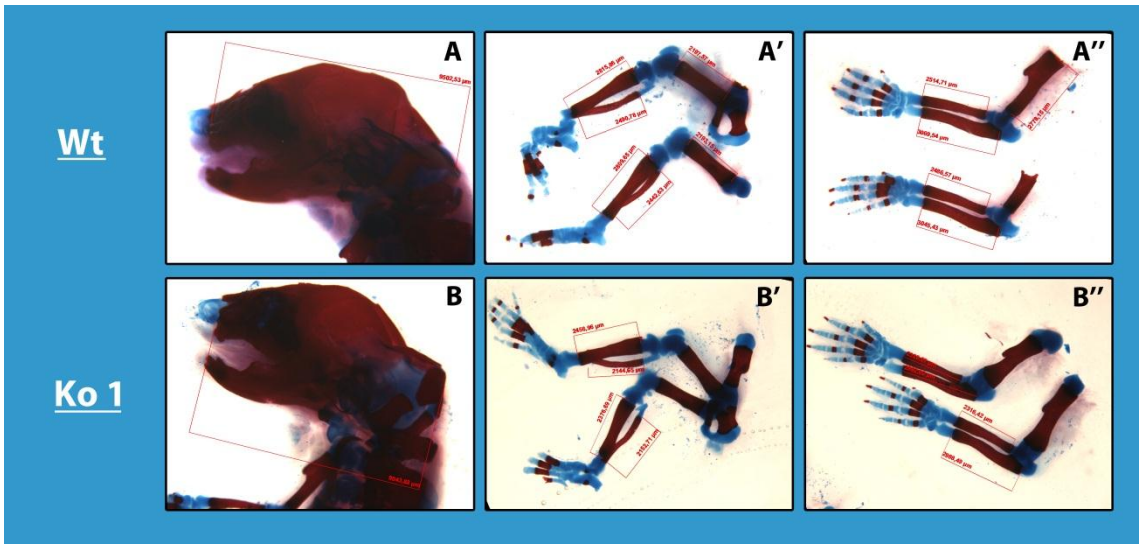

Figure 24: *Adtk1*$^{-/-}$ affects the bone length. Wild-type embryo (A-A'') and *Adtk1*$^{-/-}$ (B-B''). Skeletons staining with alzarin red and alcian blue.

4 Discussion

Previously in our lab a thorough analysis of the *Adtk1* gene was performed. From the very beginning, the expression pattern analysis suggested an important role for *Adtk1* during embryonic development.[86] This gene is expressed in the AVE at very early stages of development, at the distal tip as it starts migrating towards the anterior side.[86]

4.1 Influence of Genetic Background on Mouse Phenotypes

Characterization of genetically engineered mice requires an analysis of the gene of interest and the genetic background on which the mutation is maintained. An essential prerequisite to deciphering the genetic factors that influence the phenotype of a mutant mouse is the understanding of genetic nomenclature. [99]

The mouse genetics history, that involves the study of strain-dependent phenotype variability, shows without a doubt that the genetic background onto which a gene-targeted allele is located can cause considerable variation in genetically engineered mouse phenotype. This variation can be presented as completely different phenotypes, as variations in penetrance of phenotype, or as variable expressivity of phenotype.[100] In the literature there are described different phenotype genes for the KO of the same gene in different strains. For example, loss of *c-Abl* in C57Bl6 mice conducts to severe cardiac hyperplasia, what contributes to high lethality around the time of birth. The phenotype relies on mouse genetic background, as mutant mice deficient of c-Abl protein on several other backgrounds do not present similar defects and survive much longer.[101]

There are advantages and disadvantages in performing the first analysis of a KO mouse on a mixed genetic background.[100] In the case of *Adtk1*, in previous published work the effects of that gene on a hybrid background was analyzed and their defects studied.[86, 92, 93] However, recently in our lab after inbreeding this mutation into the C57BL6 background we were able to demonstrate the importance of this gene along the embryonic development, what was evidenced by the embryonic death in the

genotyped dissections. We have also shown the possible defects occurred in an early stage of embryonic development in pure inbred background.

Conditional mutagenesis technologies rise the options for controlling genetic background effects and also allow the study of developmental and temporal modifications in gene and protein expression and thus phenotype. However, controlling the genetic background is not always practical or feasible. Many spontaneous mutations arise on a mixed or undefined genetic background.[99]

4.2 *Adtk1* involvement in PCP pathway

In vertebrates, the PCP pathway is responsible for the regulation of convergent extension movements and neural tube closure, as well as the orientation of stereociliary bundles of sensory hair cells in the inner ear. Severe neural tube defects are also involved in the vertebrate PCP pathway. For example, the PTK7 is a novel regulator of PCP pathway in vertebrates.[89]

PTK7 is a very similar defective kinase concerning the *Adtk1* and the PTK7 has been reported to be involved in PCP. This signaling pathway seems to be essential for correct neural tube closure.[86, 89]

Recently, we have bred the *Adtk1* mutant line into the C57Bl6 inbred background. Preliminary analysis of E9.5 *Adtk1* KO embryos in this inbred background revealed severe defects associated with neural tube closure (unpublished preliminary results). This result is further supported by experiments conducted using *Xenopus leavis* where the knock-down of *Adtk1* orthologous during development induces defects on cellular migration during neural tube closure and gastrulation (M. Vitorino, unpublished). PTK7 is also responsible for defects in neural tube closure and neural crest migration during *Xenopus leavis* development.[89, 90, 102]

It is possible that the *Adtk1* is also involved in neural tube closure during vertebrate development. Indeed, knocked-down experiments using *Xenopus leavis* embryos resulted in a delay in neural tube closure (M. Vitorino, unpublished).

Moreover, similar results have been detected in mAdtk1 null embryos at stage E9.5 (unpublished). Here, we propose to conduct a detailed characterization of the role of mAdtk1 in the process of neural tube closure of mouse embryos. We will analyze markers such as Noggin, involved in telencephalon, roof plate, spinal cord, neural tube, 1st arch mesenchyme and ectoderm development;[103] BMP's required for neural tube closure[104] and Vangl2 involved in hindgut diverticulum and central nervous system development.[104] Other markers of the PCP pathway will also be tested, Vanlg2,[78] Fz3 and Fz6,[105] Dvl1-3,[106] Rhoa,[107] Rock2 and JNK2[108].

Other experiments performed in our lab with *Xenopus leavis* embryos showed any involvement of *Adtk1* orthologous in PCP signaling pathway (Marta Vitorino, unpublished). It was shown by other authors that the recruitment of dishevelled to the membrane by frizzled is essential for the activation of PCP signaling pathway.[102] We demonstrated that *Adtk1* orthologous in *Xenopus leavis* could also recruit dishevelled to the membrane begging involved in PCP pathway. (M Vitorino, unpublished)

4.3 *Adtk1* involvement in Gastrulation

When *Adtk1* KO was generated in C57Bl6 strain, no KO was born. We suspected that an intrauterine death could be occurring. Because of this hypothesis we began to dissect embryos from timed mated pregnant females at different gestation stages and started looking for intrauterine death, through the presence of empty decidua (placenta where the dead embryo is reabsorbed by the mother) in all litters dissected. Therefore we started by dissecting the E13.5, E12.5 and E10.5 in the hope of finding KO embryos at these stages but we still continued with an absence of KO embryos. Yet we continued to see empty decidua in almost all dissected females. This indicated that it was more likely that the embryos were dying earlier than the analyzed stage to date.

During the dissections it was very important to find a KO at E8.5, however few embryos were dissected at this stage. The only KO embryo that was found did not reveal to be clarifying since it was very deformed not allowing us to see the different structures that constituted the embryo. However, the mFGF8 marking was restricted to a very specific place what seemed to be very interesting. Nevertheless, this is a preliminary result that needs to be further analyzed through the dissection of more embryos at this stage.

In *Xenopus leavis*, we observed that in X*Adtk1* and X*Adtk1* knocked down embryos, the closure of the blastopore was delayed (unpublished). To observe if the same type of cell migration problems are occurring in *Adtk1*$^{-/-}$ embryos during early development, embryos at E5.5-E6.5 should be analyzed. However, until the date only two KO were found in E6.5. Nevertheless, these embryos do not seem to reveal a big difference comparing to the wild-type embryos at the same stage. So, it would be very important to analyze the migration at these stages. To assess if the proper migration of Distal Visceral Endoderm (DVE) cells to originate the AVE is occurring in *Adtk1* null mutants we should try to follow the migration of these cells during mouse development.

4.4 *Adtk1* involvement in Kidney Development

In order to access the role of *Adtk1* in mouse embryonic development, *Adtk1*$^{-/-}$ mouse have been generated, by us and others, through targeted inactivation. Reported phenotypic analysis has shown that *Adtk1* knockout mice present several abnormalities related with bone morphogenesis and differentiation and also development of other organs as lungs and intestines.[86, 92, 93]

Recently we have determined that *Adtk1* is expressed in mouse kidneys during embryonic development (from E12.5 up to birth). Moreover, preliminary analysis suggests that expression at this level is likely to be important for appropriate kidney

development. In preliminary studies using the reported *Adtk1* KO mouse in the hybrid background (C57Bl6/CBA), we observed that kidneys of *Adtk1* KO mice present an altered cortex ultra-structure (unpublished, preliminary results).

Furthermore, all analyzed *Adtk1* mutants presented larger kidneys than their wild-type littermates. Preliminary histological analysis demonstrated that *Adtk1* enlarged kidneys lack medullary structures.

Morphologically, the phenotype obtained in *Adtk1* mutant kidneys is very similar to the phenotype of *Wnt4* mutant kidneys, suggesting a potential biological role in kidney development.[109] In *Wnt4* mutant kidneys, the development of smooth muscle cells in the medullary stroma is compromised, probably due to the absence or misexpression of BMP4, which occurs in those mutants; furthermore, it is already known that wnt4 in involved in controlling mesenchyme to epithelium transformation that underlies nephron development and null mutants for this gene fail to pretubular cell aggregates, thus failing tubule induction.[67, 110]

The kidney development is a process not yet fully understood. It is known that molecules from several signaling pathways are involved in the formation of the kidney, however, their relative positions in the pathways remain unclear and intermediate players remain unknown. Additionally, Wnt proteins are known to play important roles in the growth and morphogenesis of organs such as the kidney and lungs, in the regulation of branching morphogenesis.[111]

4.5 *Adtk1* involvement in Bone Formation

The formation of bone is a continuous process in vertebrate development, initiated at embryogenesis and persisting after birth with growth, (re)modeling and fracture repair.[7]

The subsequent processes of either fetal bone growth, postnatal growth or pubertal growth are finely orchestrated by transcription factors, consecutive signaling

pathways and controlled by feedback loops or other molecular processes. Many genes play a role in this process, such as transcription factors, growth factors, hormones, receptors, cell-cycle regulators and signal transducers.[112] The curated Gene Ontology Database (http://www.geneontology.org/) lists 151 genes associated with skeletal development.

Data presented by Imuta, et. al. (2009), showed that *Adtk1* (*Pkdcc*) knockout mice exhibited shorter limbs than its wild-type littermates. *Adtk1* mutant specimens analyzed for its skeleton also presented differences in bone length,[86] although mild ones comparing to Imuta (2009).

Reported bone defects in *Pkdcc* mutants,[92] however, until now all null mutants obtained were roughly the same size as its wild-type littermates and no obvious differences were noticed. However, skeletal analysis with alizarin red and alcian blue provided further and more detailed information. In these limbs, the mineralized regions, which stained red with alizarin red, were significantly shortened compared with its wild type littermates, whereas the size and morphology of the cartilage, which stained blue with alcian blue, were not significantly affected.

5 Future Perspectives

At the end of this Master thesis, some of our initial questions were answered while others remained without an answer. At this moment, we thought that some questions are cleared and there is still a lot of work to be done starting from these preliminary data.

In this thesis it was reported that *Adtk1*$^{-/-}$ embryos present several defects during kidney development. Our preliminary analyses have shown that this gene is expressed in the developing kidney. To better unveil the requirement of *Adtk1* during mouse kidney development, an in-depth analysis of the phenotypes displayed by the reported *Adtk1* KO mouse in the hybrid background (C57Bl6/DBA) should be analyzed.

Furthermore, *Adtk1*$^{-/-}$ and wild-type mouse embryos should be dissected and the kidneys collected for study at the early (E12.5) and more advanced stages of maturation (up to birth). A detailed pattern of expression of *Adtk1* during mouse kidney development should also be performed, since the *in situ* hybridization results performed for the *Adtk1* gene and kidneys markers were not conclusive. Histological sections should be performed to determine the expression of all these markers in KO and wild-type embryos. The expression of these markers would be compared with published data and the structure and cellular organization of the tissues and organ would be assessed to identify specific abnormalities in kidney organogenesis.

Adtk1 is also involved in neural tube closure during mouse development as detected in m*Adtk1* null embryos at stage E9.5. It would be interesting to conduct a detailed characterization of the role of m*Adtk1* in the process of neural tube closure of mouse embryos. In future, using the *Adtk*$^{-/-}$ mouse embryo, we aim to perform a detailed characterization of genes required for neural tube closure for this end, WISH, immunohistochemistry and histology techniques will be employed in embryos ranging from E8.5 and E9.5.

It would also be interesting to analyze markers such as Noggin, involved in telencephalon, roofplate, spinal cord, neural tube, 1st arch mesenchyme and ectoderm development.[103] Other markers of the PCP pathway should also be tested, Vanlg2,[78] Fz3 and Fz6,[105] Dvl1-3,[106] Rhoa,[107] Rock2 and JNK2[108]. In addition, histological techniques would be applied to explore in further detail the alterations arising from *Adtk1* KO. This study would provide new insights on the regulatory pathways and morphogenetic mechanisms in which this gene might be involved.

Preliminary results using *Adtk1*$^{-/-}$ mutants in an inbred background showed that these null mutants are dying in uterus during gestation. As such, in the future we should investigate abnormalities during embryonic development and characterize the expression pattern of several markers of primitive streak, mesoderm and endoderm using whole mount *in situ* hybridization and histological analyses. WISH should be performed using several AVE markers such as *Cer1*, *Dkk1*, *Lim1* and *Lefty1*[25, 113] and primitive streak markers such as *FGF8*, *Celsr1*, *Fst*.[79, 114, 115] In addition, these mouse embryos should be sectioned in order to access in more detail the pattern of expression at the histological level to identify alterations at the level of the tissues structure.

In addition, knocked-down of *Adtk1* orthologue in developing *Xenopus leavis* embryos resulted in gastrulation defects due to atypical cellular migration. To observe if a similar defect is observed in null mouse, a complete and integrated study during mouse peri-gastrulation stages (E5.5-E7.5) should be performed, including AVE migration. To assess if the proper migration of Distal Visceral Endoderm (DVE) cells to originate the AVE is occurring in *Adtk1* null mutants we would try to follow the migration of these cells during mouse development. With this purpose we would use the transgenic line Cer1P-GFP [116] that allows to easy visualize the position of the AVE.

Appendix

List of Solutions	
Solutions	Composition
Pre-hybridization solution in WISH	50% formamide 5X SSC 0,1% Tween-20 50µg/ml heparin Prepare it with DEPC treated water
Hybridization solution in WISH	Pre-hybridization solution: 50µg/ml tRNA 50µg/ml salmon sperm DNA (ssDNA) denatured probe
WISH solution I	50% formamide 4X SSC 1% SDS H2O
WISH solution II	50% formamide 2X SSC H2O
SSC 20x	3M NaCl 0.3M Na3C3H5O(CO2)3 (sodium citrate) Fill with water and adjust pH to 7.0
MABT	150mM NaCl 100mM C4H4O4 (Maleic Acid) 0.1% Tween-20 Fill with water and adjust pH to 7.5
NTMT	0.1M NaCl 0.1M Tris-HCl 0.05M MgCl2

	0.1% Tween-20
	Fill with water
PBS 10x	80.6mM Na3PO4 (sodium phosphate) 19.4mM KH2PO4 (potassium phosphate) 27mM KCl 1.37M NaCl Fill with water and adjust pH to 7.4

List of *in situ hybridization* probes

Clone	Enzyme	RNA Polymerase
ADTK	Not I	T3
Fgf8	Not I	T7
Wnt4	BamHI	T7
c-RET	BamHI	T7
Noggin	Not I	T7

List of PK time during *in situ* hybridization

Embryos E7.5	5 min
Embryos E8.5	7 min
Embryos E9.5	8min
Embryos E10.5	9 min
Embryos E11.5	10 min
Kidney E12.5	7 min
Kidney E13.5	8 min
Kidney E 14.5	9 min
Kidney E15.5	11min

References:

1. Gilbert, S.F., *Developmental Biology*. Ninth Edition ed. 2010: Sinauer Associates, Inc.
2. Jamsai, D. and M.K. O'Bryan, *Mouse models in male fertility research.* Asian J Androl, 2011. **13**(1): p. 139-151.
3. Rossant, J., *Developmental biology: A mouse is not a cow.* Nature, 2011. **471**(7339): p. 457-458.
4. Jackson, I.J. and C.M. Abbott, *Mouse Genetics and Transgenics*

A Practical Approach. 2000: Oxford University.
5. Bedell, M.A., N.A. Jenkins, and N.G. Copeland, *Mouse models of human disease. Part I: techniques and resources for genetic analysis in mice.* Genes & Development, 1997. **11**(1): p. 1-10.
6. Bedell, M.A., et al., *Mouse models of human disease. Part II: recent progress and future directions.* Genes & Development, 1997. **11**(1): p. 11-43.
7. Rossant, J. and P.P.L. Tam, *Mouse Development*

Patterning, Morphogenesis, and Organogenesis. 2002: Academic Press. 712.
8. Slack, J.M.W., *Essential Developmental Biology*. 2ª Edition ed. 2006: Blackweel Publishing.
9. Zernicka-Goetz, M., *Patterning of the embryo: the first spatial decisions in the life of a mouse.* Development, 2002. **129**(4): p. 815-829.
10. Gardner, R.L., *The early blastocyst is bilaterally symmetrical and its axis of symmetry is aligned with the animal-vegetal axis of the zygote in the mouse.* Development, 1997. **124**(2): p. 289-301.
11. Beddington, R.S.P. and E.J. Robertson, *Axis Development and Early Asymmetry in Mammals.* Cell, 1999. **96**(2): p. 195-209.
12. Inman, K.E. and K.M. Downs, *The murine allantois: emerging paradigms in development of the mammalian umbilical cord and its relation to the fetus.* genesis, 2007. **45**(5): p. 237-258.
13. Piko, L. and K.B. Clegg, *Quantitative changes in total RNA, total poly(A), and ribosomes in early mouse embryos.* Developmental Biology, 1982. **89**(2): p. 362-378.
14. Wang, H. and S.K. Dey, *Roadmap to embryo implantation: clues from mouse models.* Nat Rev Genet, 2006. **7**(3): p. 185-199.
15. Dey, S.K., et al., *Molecular Cues to Implantation.* Endocrine Reviews, 2004. **25**(3): p. 341-373.
16. Zernicka-Goetz, M., *Proclaiming fate in the early mouse embryo.* Nat Cell Biol, 2011. **13**(2): p. 112-114.
17. Loebel, D.A.F., et al., *Lineage choice and differentiation in mouse embryos and embryonic stem cells.* Developmental Biology, 2003. **264**(1): p. 1-14.
18. Wells, J.M. and D.A. Melton, *VERTEBRATE ENDODERM DEVELOPMENT.* Annual Review of Cell and Developmental Biology, 1999. **15**(1): p. 393-410.

19. Tam, P.P.L. and D.A.F. Loebel, *Gene function in mouse embryogenesis: get set for gastrulation.* Nat Rev Genet, 2007. **8**(5): p. 368-381.
20. Rashbass, P., et al., *A cell autonomous function of Brachyury in T/T embryonic stem cell chimaeras.* Nature, 1991. **353**(6342): p. 348-351.
21. Lee, J.D. and K.V. Anderson, *Morphogenesis of the node and notochord: The cellular basis for the establishment and maintenance of left–right asymmetry in the mouse.* Developmental Dynamics, 2008. **237**(12): p. 3464-3476.
22. Beddington, R.S., *Induction of a second neural axis by the mouse node.* Development, 1994. **120**(3): p. 613-620.
23. Lawson, K.A., J.J. Meneses, and R.A. Pedersen, *Clonal analysis of epiblast fate during germ layer formation in the mouse embryo.* Development, 1991. **113**(3): p. 891-911.
24. Thomas, P. and R. Beddington, *Anterior primitive endoderm may be responsible for patterning the anterior neural plate in the mouse embryo.* Current biology : CB, 1996. **6**(11): p. 1487-1496.
25. Belo JA, et al., *Cerberus-like is a secreted factor with neutralizing activity expressed in the anterior primitive endoderm of the mouse gastrula.* Mech Dev., 1997. **68**: p. 45-57.
26. Rosenquist, T.A. and G.R. Martin, *Visceral endoderm-1 (VE-1): an antigen marker that distinguishes anterior from posterior embryonic visceral endoderm in the early post-implantation mouse embryo*. Vol. 49. 1995. 117-21.
27. Simeone, A., et al., *Retinoic acid induces stage-specific antero-posterior transformation of rostral central nervous system.* Mechanisms of Development, 1995. **51**(1): p. 83-98.
28. Ang, S.-L. and J. Rossant, *HNF-3² is essential for node and notochord formation in mouse development.* Cell, 1994. **78**(4): p. 561-574.
29. Thomas, P.Q., A. Brown, and R.S. Beddington, *Hex: a homeobox gene revealing peri-implantation asymmetry in the mouse embryo and an early transient marker of endothelial cell precursors.* Development, 1998. **125**(1): p. 85-94.
30. Dunwoodie, S.L., T.A. Rodriguez, and R.S.P. Beddington, *Msg1 and Mrg1, founding members of a gene family, show distinct patterns of gene expression during mouse embryogenesis.* Mechanisms of Development, 1998. **72**(1-2): p. 27-40.
31. Rossant, J. and P.P.L. Tam, *Blastocyst lineage formation, early embryonic asymmetries and axis patterning in the mouse.* Development, 2009. **136**(5): p. 701-713.
32. Belo, J.A., et al., *Cerberus-like is a secreted BMP and nodal antagonist not essential for mouse development.* genesis, 2000. **26**(4): p. 265-270.
33. Schier, A.F., *NODAL SIGNALING IN VERTEBRATE DEVELOPMENT.* Annual Review of Cell and Developmental Biology, 2003. **19**(1): p. 589-621.
34. Caraci, F., et al., *The Wnt Antagonist, Dickkopf-1, as a Target for the Treatment of Neurodegenerative Disorders.* Neurochemical Research, 2008. **33**(12): p. 2401-2406.

35. Tam, P.P. and K.A. Steiner, *Anterior patterning by synergistic activity of the early gastrula organizer and the anterior germ layer tissues of the mouse embryo.* Development, 1999. **126**(22): p. 5171-5179.
36. Stottmann, R.W., R.M. Anderson, and J. Klingensmith, *The BMP Antagonists Chordin and Noggin Have Essential but Redundant Roles in Mouse Mandibular Outgrowth.* Developmental Biology, 2001. **240**(2): p. 457-473.
37. Dressler, G.R., *The Cellular Basis of Kidney Development.* Annual Review of Cell and Developmental Biology, 2006. **22**(1): p. 509-529.
38. Cebrián, C., et al., *Morphometric index of the developing murine kidney.* Developmental Dynamics, 2004. **231**(3): p. 601-608.
39. Grobstein, C., *Trans-filter induction of tubules in mouse metanephrogenic mesenchyme.* Experimental Cell Research, 1956. **10**(2): p. 424-440.
40. Boyle, S. and M. de Caestecker, *Role of transcriptional networks in coordinating early events during kidney development.* American Journal of Physiology - Renal Physiology, 2006. **291**(1): p. F1-F8.
41. Grieshammer, U., et al., *SLIT2-Mediated ROBO2 Signaling Restricts Kidney Induction to a Single Site.* Developmental Cell, 2004. **6**(5): p. 709-717.
42. Hellmich, H.L., et al., *Embryonic expression of glial cell-line derived neurotrophic factor (GDNF) suggests multiple developmental roles in neural differentiation and epithelial-mesenchymal interactions.* Mechanisms of Development, 1996. **54**(1): p. 95-105.
43. Pichel, J.G., et al., *Defects in enteric innervation and kidney development in mice lacking GDNF.* Nature, 1996. **382**(6586): p. 73-76.
44. Baloh, R.H., et al., *TrnR2, a Novel Receptor That Mediates Neurturin and GDNF Signaling through Ret.* Neuron, 1997. **18**(5): p. 793-802.
45. Pachnis, V., B. Mankoo, and F. Costantini, *Expression of the c-ret proto-oncogene during mouse embryogenesis.* Development, 1993. **119**(4): p. 1005-1017.
46. Sainio, K., et al., *Differential regulation of two sets of mesonephric tubules by WT-1.* Development, 1997. **124**(7): p. 1293-1299.
47. Tanaka, M., H. Xiao, and K. Kiuchi, *Heparin facilitates glial cell line-derived neurotrophic factor signal transduction.* NeuroReport, 2002. **13**(15): p. 1913-1916.
48. Cacalano, G., et al., *GFR[alpha]1 Is an Essential Receptor Component for GDNF in the Developing Nervous System and Kidney.* Neuron, 1998. **21**(1): p. 53-62.
49. Maeshima, A., *Label-retaining cells in the kidney: origin of regenerating cells after renal ischemia.* Clinical and Experimental Nephrology, 2007. **11**(4): p. 269-274.
50. Moore, M.W., et al., *Renal and neuronal abnormalities in mice lacking GDNF.* Nature, 1996. **382**(6586): p. 76-79.
51. Sanchez, M.P., et al., *Renal agenesis and the absence of enteric neurons in mice lacking GDNF.* Nature, 1996. **382**(6586): p. 70-73.

52. Brophy, P.D., et al., *Regulation of ureteric bud outgrowth by Pax2-dependent activation of the glial derived neurotrophic factor gene.* Development, 2001. **128**(23): p. 4747-4756.
53. Sainio, K., et al., *Glial-cell-line-derived neurotrophic factor is required for bud initiation from ureteric epithelium.* Development, 1997. **124**(20): p. 4077-4087.
54. Andrews, W., et al., *The role of Slit-Robo signaling in the generation, migration and morphological differentiation of cortical interneurons.* Developmental Biology, 2008. **313**(2): p. 648-658.
55. Costantini, F. and R. Shakya, *GDNF/Ret signaling and the development of the kidney.* BioEssays, 2006. **28**(2): p. 117-127.
56. Batourina, E., et al., *Vitamin A controls epithelial/mesenchymal interactions through Ret expression.* Nat Genet, 2001. **27**(1): p. 74-78.
57. Mendelsohn, C., et al., *Stromal cells mediate retinoid-dependent functions essential for renal development.* Development, 1999. **126**(6): p. 1139-1148.
58. Srinivas, S., et al., *Dominant effects of RET receptor misexpression and ligand-independent RET signaling on ureteric bud development.* Development, 1999. **126**(7): p. 1375-1386.
59. Schuchardt, A., et al., *Defects in the kidney and enteric nervous system of mice lacking the tyrosine kinase receptor Ret.* Nature, 1994. **367**(6461): p. 380-383.
60. Dudley, A.T. and E.J. Robertson, *Overlapping expression domains of bone morphogenetic protein family members potentially account for limited tissue defects in BMP7 deficient embryos.* Developmental Dynamics, 1997. **208**(3): p. 349-362.
61. Miyazaki, Y., et al., *Evidence that bone morphogenetic protein 4 has multiple biological functions during kidney and urinary tract development.* Kidney Int, 2003. **63**(3): p. 835-844.
62. Winnier, G., et al., *Bone morphogenetic protein-4 is required for mesoderm formation and patterning in the mouse.* Genes & Development, 1995. **9**(17): p. 2105-2116.
63. Michos, O., et al., *Reduction of BMP4 activity by gremlin 1 enables ureteric bud outgrowth and GDNF/WNT11 feedback signalling during kidney branching morphogenesis.* Development, 2007. **134**(13): p. 2397-2405.
64. Moriyama, A., et al., *GFP transgenic mice reveal active canonical Wnt signal in neonatal brain and in adult liver and spleen.* genesis, 2007. **45**(2): p. 90-100.
65. Bridgewater, D., et al., *Canonical WNT/β-catenin signaling is required for ureteric branching.* Developmental Biology, 2008. **317**(1): p. 83-94.
66. Merkel, C., C. Karner, and T. Carroll, *Molecular regulation of kidney development: is the answer blowing in the Wnt?* Pediatric Nephrology, 2007. **22**(11): p. 1825-1838.
67. Stark, K., et al., *Epithelial transformation of metanephric mesenchyme in the developing kidney regulated by Wnt-4.* Nature, 1994. **372**(6507): p. 679-683.
68. Carroll, T.J., et al., *Wnt9b Plays a Central Role in the Regulation of Mesenchymal to Epithelial Transitions Underlying Organogenesis of the Mammalian Urogenital System.* Developmental Cell, 2005. **9**(2): p. 283-292.

69. Dressler, G.R., *Advances in early kidney specification, development and patterning.* Development, 2009. **136**(23): p. 3863-3874.
70. Bassuk, A.G. and Z. Kibar, *Genetic Basis of Neural Tube Defects.* Seminars in Pediatric Neurology, 2009. **16**(3): p. 101-110.
71. Copp, A.J., N.D.E. Greene, and J.N. Murdoch, *The genetic basis of mammalian neurulation.* Nat Rev Genet, 2003. **4**(10): p. 784-793.
72. Van Allen, M.I., et al., *Evidence for multi-site closure of the neural tube in humans.* American Journal of Medical Genetics, 1993. **47**(5): p. 723-743.
73. Karamboulas, K., H.J. Dranse, and T.M. Underhill, *Regulation of BMP-dependent chondrogenesis in early limb mesenchyme by TGFβ signals.* Journal of Cell Science, 2010. **123**(12): p. 2068-2076.
74. Morriss-Kay, G.M. and A.O.M. Wilkie, *Growth of the normal skull vault and its alteration in craniosynostosis: insights from human genetics and experimental studies.* Journal of Anatomy, 2005. **207**(5): p. 637-653.
75. Copp, A.J., *Neurulation in the cranial region – normal and abnormal.* Journal of Anatomy, 2005. **207**(5): p. 623-635.
76. Wallingford, J.B. and R.M. Harland, *Neural tube closure requires Dishevelled-dependent convergent extension of the midline.* Development, 2002. **129**(24): p. 5815-5825.
77. Borovina, A., et al., *Vangl2 directs the posterior tilting and asymmetric localization of motile primary cilia.* Nat Cell Biol, 2010. **12**(4): p. 407-412.
78. Shafer, B., et al., *Vangl2 Promotes Wnt/Planar Cell Polarity-like Signaling by Antagonizing Dvl1-Mediated Feedback Inhibition in Growth Cone Guidance.* Developmental Cell, 2011. **20**(2): p. 177-191.
79. Hadjantonakis, A.-K., et al., *Celsr1, a Neural-Specific Gene Encoding an Unusual Seven-Pass Transmembrane Receptor, Maps to Mouse Chromosome 15 and Human Chromosome 22qter.* Genomics, 1997. **45**(1): p. 97-104.
80. Hashimoto, M. and H. Hamada, *Translation of anterior-posterior polarity into left-right polarity in the mouse embryo.* Current Opinion in Genetics & Development, 2010. **20**(4): p. 433-437.
81. Ybot-Gonzalez, P., et al., *Neural plate morphogenesis during mouse neurulation is regulated by antagonism of Bmp signalling.* Development, 2007. **134**(17): p. 3203-3211.
82. Murdoch, J.N. and A.J. Copp, *The relationship between sonic Hedgehog signaling, cilia, and neural tube defects.* Birth Defects Research Part A: Clinical and Molecular Teratology, 2010. **88**(8): p. 633-652.
83. Soo, K., et al., *Twist Function Is Required for the Morphogenesis of the Cephalic Neural Tube and the Differentiation of the Cranial Neural Crest Cells in the Mouse Embryo.* Developmental Biology, 2002. **247**(2): p. 251-270.
84. Harris, M.J. and D.M. Juriloff, *An update to the list of mouse mutants with neural tube closure defects and advances toward a complete genetic perspective of neural tube closure.* Birth Defects Research Part A: Clinical and Molecular Teratology, 2010. **88**(8): p. 653-669.

85. Massa, V., et al., *Apoptosis is not required for mammalian neural tube closure.* Proceedings of the National Academy of Sciences, 2009. **106**(20): p. 8233-8238.
86. Gonçalves, L., et al., *Identification and functional analysis of novel genes expressed in the Anterior Visceral Endoderm.* The International Journal of Developmental Biology

2011. **55**

p. 281-295.
87. Bejsovec, A., *Wnt Pathway Activation: New Relations and Locations.* Cell, 2005. **120**(1): p. 11-14.
88. Kroiher, M., M.A. Miller, and R.E. Steele, *Deceiving appearances: signaling by "dead" and "fractured" receptor protein-tyrosine kinases.* BioEssays, 2001. **23**(1): p. 69-76.
89. Lu, X., et al., *PTK7/CCK-4 is a novel regulator of planar cell polarity in vertebrates.* Nature, 2004. **430**(6995): p. 93-98.
90. Yen, W.W., et al., *PTK7 is essential for polarized cell motility and convergent extension during mouse gastrulation.* Development, 2009. **136**(12): p. 2039-2048.
91. Bento, M., et al., *Identification of differentially expressed genes in the heart precursor cells of the chick embryo.* Gene Expression Patterns, 2011. **11**(7): p. 437-447.
92. Imuta, Y., et al., *Short limbs, cleft palate, and delayed formation of flat proliferative chondrocytes in mice with targeted disruption of a putative protein kinase gene, Pkdcc (AW548124).* Developmental Dynamics, 2009. **238**(1): p. 210-222.
93. Kinoshita, M., et al., *The novel protein kinase Vlk is essential for stromal function of mesenchymal cells.* Development, 2009. **136**(12): p. 2069-2079.
94. Suda, Y., et al., *Functional equivalency between Otx2 and Otx1 in development of the rostral head.* Development, 1999. **126**(4): p. 743-757.
95. Lin, W., et al., *Cloning of the mouse Sef gene and comparative analysis of its expression with Fgf8 and Spry2 during embryogenesis.* Mechanisms of Development, 2002. **113**(2): p. 163-168.
96. Yagi, T., et al., *A Novel ES Cell Line, TT2, with High Germline-Differentiating Potency.* Analytical Biochemistry, 1993. **214**(1): p. 70-76.
97. Clarke, J.C., et al., *Regulation of c-Ret in the developing kidney is responsive to Pax2 gene dosage.* Human Molecular Genetics, 2006. **15**(23): p. 3420-3428.
98. Naylor, R.W. and E.A. Jones, *Notch activates Wnt-4 signalling to control medio-lateral patterning of the pronephros.* Development, 2009. **136**(21): p. 3585-3595.
99. Linder, C., *Genetic variables that influence phenotype.* ILAR Jornal-National Research Council, Institute of Laboratory Animal Resources, 2006. **47**: p. 132-140.

100. Doetschman, T., *Influence of Genetic Background on Genetically Engineered Mouse Phenotypes*, in *Gene Knockout Protocols*, S. Edition, Editor. 2009, Humana Press.
101. Qiu, Z., Y. Cang, and S.P. Goff, *c-Abl tyrosine kinase regulates cardiac growth and development.* Proceedings of the National Academy of Sciences, 2010. **107**(3): p. 1136-1141.
102. Shnitsar, I. and A. Borchers, *PTK7 recruits dsh to regulate neural crest migration.* Development, 2008. **135**(24): p. 4015-4024.
103. Valenzuela, D., et al., *Identification of mammalian noggin and its expression in the adult nervous system.* The Journal of Neuroscience, 1995. **15**(9): p. 6077-6084.
104. Zhao, G.-Q., *Consequences of knocking out BMP signaling in the mouse.* genesis, 2003. **35**(1): p. 43-56.
105. Montcouquiol, M., et al., *Asymmetric Localization of Vangl2 and Fz3 Indicate Novel Mechanisms for Planar Cell Polarity in Mammals.* The Journal of Neuroscience, 2006. **26**(19): p. 5265-5275.
106. Hashimoto, M. and H. Hamada, *Translation of anterior–posterior polarity into left–right polarity in the mouse embryo.* Current Opinion in Genetics & Development, 2010. **20**(4): p. 433-437.
107. Caddy, J., et al., *Epidermal Wound Repair Is Regulated by the Planar Cell Polarity Signaling Pathway.* Developmental Cell, 2010. **19**(1): p. 138-147.
108. Kuan, C.-Y., et al., *The Jnk1 and Jnk2 Protein Kinases Are Required for Regional Specific Apoptosis during Early Brain Development.* Neuron, 1999. **22**(4): p. 667-676.
109. Itäranta, P., et al., *Wnt-4 signaling is involved in the control of smooth muscle cell fate via Bmp-4 in the medullary stroma of the developing kidney.* Developmental Biology, 2006. **293**(2): p. 473-483.
110. Kispert, A., S. Vainio, and A.P. McMahon, *Wnt-4 is a mesenchymal signal for epithelial transformation of metanephric mesenchyme in the developing kidney.* Development, 1998. **125**(21): p. 4225-4234.
111. Bridgewater, D. and N. Rosenblum, *Stimulatory and inhibitory signaling molecules that regulate renal branching morphogenesis.* Pediatric Nephrology, 2009. **24**(9): p. 1611-1619.
112. Christine, H., *Transcriptional networks controlling skeletal development.* Current Opinion in Genetics & Development, 2009. **19**(5): p. 437-443.
113. Glinka, A., et al., *Head induction by simultaneous repression of Bmp and Wnt signalling in Xenopus.* Nature, 1997. **389**(6650): p. 517-519.
114. Tanaka, A., et al., *Cloning and characterization of an androgen-induced growth factor essential for the androgen-dependent growth of mouse mammary carcinoma cells.* Proceedings of the National Academy of Sciences, 1992. **89**(19): p. 8928-8932.
115. Nakamura, T., et al., *Activin-binding protein from rat ovary is follistatin.* Science, 1990. **247**(4944): p. 836-838.

116. Mesnard, D., et al., *The Anterior-Posterior Axis Emerges Respecting the Morphology of the Mouse Embryo that Changes and Aligns with the Uterus before Gastrulation.* Current biology : CB, 2004. **14**(3): p. 184-196.